J. Kunisawa and H. Kiyono	Alcaligenes is commensal bacteria habituating in the gut-associated lymphoid tissue for the regulation of intestinal IgA responses	Front in Immunol	3	1	2012
J. Kunisawa and H. Kiyono	Immunological function of sphingosine 1-phosphate in the intestine	Nutrients	4	154	2012
J. Kunisawa and H. Kiyono	Peaceful mutualism in the gut: Revealing key commensal bacteria for the creation and maintenance of immunological homeostasis	Cell Host Microbe	9	83	2011
H. Kayamuro, Y. Yoshioka, Y. Abe, S. Arita, K. Katayama, T. Nomura, T. Yoshikawa, R. Kubota-Koketsu, K. Ikuta, S. Okamoto, Y. Mori, J. Kunisawa, H. Kiyono, N. Itoh, K. Nagano, H. Kamada, Y. Tsutsumi, S. I. Tsunoda	Interleukin-1 family cytokines as mucosal vaccine adjuvants for induction of protective immunity against influenza virus	J Virol	84	12703	2010
T. Obata, Y. Goto, J. Kunisawa, S. Sato, M. Sakamoto, H. Setoyama, T. Matsuki, K. Nonaka, N. Shibata, M. Gohda, Y. Kagiyama, T. Nochi, Y. Yuki, Y. Fukuyama, A. Mukai, S. Shinzaki, K. Fujihashi, C. Sasakawa, H. Iijima, M. Goto, Y. Umesaki, Y. Benno, and H. Kiyono	Indigenous opportunistic bacteria inhabit mammalian gut-associated lymphoid tissues and share a mucosal antibody-mediated symbiosis	Proc Natl Acad Sci USA	107	7419	2010
Men TT, Huy NT, Trang DT, Shuaibu MN, Hirayama K, Kamei K	A simple and inexpensive haemozoin-based colorimetric method to evaluate anti-malarial drug activity	Malar J	11	e272-	2012

Hindawi Publishing Corporation
Evidence-Based Complementary and Alternative Medicine
Volume 2013, Article ID 148297, 11 pages
http://dx.doi.org/10.1155/2013/148297

Research Article

Enhancement of Lymphangiogenesis *In Vitro* via the Regulations of HIF-1α Expression and Nuclear Translocation by Deoxyshikonin

Orawin Prangsaengtong,[1,2] Jun Yeon Park,[1] Akiko Inujima,[1] Yoshiko Igarashi,[1] Naotoshi Shibahara,[1] and Keiichi Koizumi[1]

[1] *Department of Kampo Diagnostics, Institute of Natural Medicine, University of Toyama, Toyama 930-0194, Japan*
[2] *Department of Biopharmacy, Faculty of Pharmacy, Srinakharinwirot University, Nakhonnayok 26120, Thailand*

Correspondence should be addressed to Keiichi Koizumi; kkoizumi@inm.u-toyama.ac.jp

Received 11 January 2013; Revised 19 March 2013; Accepted 21 March 2013

Academic Editor: Ken Yasukawa

The objectives of this study were to determine the effects of deoxyshikonin on lymphangiogenesis. Deoxyshikonin enhanced the ability of human dermal lymphatic microvascular endothelial cells (HMVEC-dLy) to undergo time-dependent *in vitro* cord formation. Interestingly, an opposite result was observed in cells treated with shikonin. The increased cord formation ability following deoxyshikonin treatment correlated with increased VEGF-C mRNA expression to higher levels than seen for VEGF-A and VEGF-D mRNA expression. We also found that deoxyshikonin regulated cord formation of HMVEC-dLy by increasing the HIF-1α mRNA level, HIF-1α protein level, and the accumulation of HIF-1α in the nucleus. Knockdown of the HIF-1α gene by transfection with siHIF-1α decreased VEGF-C mRNA expression and cord formation ability in HMVEC-dLy. Deoxyshikonin treatment could not recover VEGF-C mRNA expression and cord formation ability in HIF-1α knockdown cells. This indicated that deoxyshikonin induction of VEGF-C mRNA expression and cord formation in HMVEC-dLy on Matrigel occurred mainly via HIF-1α regulation. We also found that deoxyshikonin promoted wound healing *in vitro* by the induction of HMVEC-dLy migration into the wound gap. This study describes a new effect of deoxyshikonin, namely, the promotion of cord formation by human endothelial cells via the regulation of HIF-1α. The findings suggest that deoxyshikonin may be a new drug candidate for wound healing and treatment of lymphatic diseases.

1. Introduction

Lymphangiogenesis is similar to angiogenesis and refers to the formation of lymphatic vessels from preexisting lymphatic vessels, which play an important role in tissue-fluid homeostasis, as a tissue drainage system, immunosurveillance, and absorption of dietary fat [1]. Dysfunction of lymphatic vessels leads to chronic edema and impairment of immune responses. In adult tissue, the induction of new lymphatic vessel growth also promotes inflammation, wound healing, and tumor metastasis to the lymph node [2]. The molecular mechanisms of angiogenesis and its treatment are already well known, whereas understanding of the functions and regulatory pathways of lymphangiogenesis and its treatment has been far less explored [1].

Vascular endothelial growth factors (VEGFs) are interesting inducers of lymphangiogenesis, because they are a highly specific mitogen for endothelial cells [3] and transcriptional factors; hypoxia-inducible factor-1 (HIF-1), which is composed of two subunits, HIF-1alpha (HIF-1α) and HIF-1beta (HIF-1β) [4, 5], can modulate VEGF gene expression [6–8]; however, the role of these regulators in the lymphangiogenesis process is poorly understood.

Shiunko is a typical Kampo drug ointment (a traditional botanic formula) used for the treatment of burns and wounds in Japan [9, 10]. Shiunko has been proved

to improve wound healing by promoting reepithelialization and granulation tissue formation, including angiogenesis [10]; however, there are on reports of the effect of shiunko on lymphangiogenesis. Lymphangiogenesis and angiogenesis are important processes in wound healing [11] and the efficacy of shiunko for the promotion of lymphangiogenesis and also angiogenesis in wound healing may be derived from the effect of components of this herbal medicine.

One of the components of shiunko is Lithospermi Radix (LR, the dried root of *Lithospermum erythrorhizon* Sieb. et Zucc, also called Zicao or Gromwell) that contains several compounds of shikonin and its derivatives, such as deoxyshikonin, acetylshikonin, isobutylshikonin, and others [12]; however, there is no report on shikonin and its derivatives that promote lymphangiogenesis or angiogenesis. In contrast, we found that shikonin and some derivatives have strongly shown to inhibit angiogenesis in *in vitro* and *in vivo* models [9] by suppressing VEGF production, proliferation, and the migration of endothelial cells [13]. These compounds also blocked integrin $\alpha v\beta 3$ expression and inhibited B16 melanoma- and tumor necrosis factor-alpha-induced angiogenesis in mice [9]. To find another shikonin derivative that may have an effect on angiogenesis and lymphangiogenesis, deoxyshikonin was examined in this study. Because traditional medicine for lymphangiogenesis treatment has not been explored widely, this study attempted to find a new mechanism of this compound for controlling lymphangiogenesis *in vitro*.

2. Materials and Methods

2.1. Materials. Deoxyshikonin was purchased from Tokyo Chemical Industry (TCI) (Tokyo, Japan). The compounds were dissolved in dimethylsulfoxide (DMSO) to make a stock solution. Matrigel was purchased from BD Biosciences (San Diego, CA, USA). HIF-1α siRNA and the antibodies against HIF-1α and PCNA were purchased from Santa Cruz Biotechnology, Inc. (Santa Cruz, CA, USA). Polyclonal rabbit anti-mouse immunoglobulin/HRP, polyclonal goat anti-rabbit immunoglobulin/HRP, and polyclonal swine anti-rabbit immunoglobulins/FITC were purchased from Dako (Glostrup, Denmark). Dynabeads protein G was purchased from Invitrogen (Oslo, Norway). Vectashield mounting medium with DAPI was from Vector Laboratories, Inc. (Burlingame, CA, USA). Rhodamine phalloidin was obtained from Life Technologies (Carlsbad, CA, USA). The culture inserts were from Ibidi (Martinsried, Germany).

2.2. Endothelial Cells. Human dermal lymphatic microvascular endothelial cells (HMVEC-dLy) and human dermal microvascular endothelial cells (HMVEC-d) were obtained from Takara Bio Inc. (Shiga, Japan). The cells were primary culture cells. Cells were cultured in Clonetics EGM-2 MV Bullet Kit (Takara Bio) in a humidified atmosphere (5% CO_2, 95% air). Cells were passaged upon reaching confluence with Trypsin-EDTA solution. To maintain normal growth, the primary cells from 5th to 15th passages were used in the study.

2.3. Proliferation Assay. Cell viability after treatment with various concentrations of deoxyshikonin and shikonin was assessed with a WST-8 cell proliferation assay kit (DOJINDO, Kumamoto, Japan). Cells were cultured in 96-well plates at 37°C. At the time of measurement, 10 μL WST-8 reagent was added to each well and the cells were cultured continuously for 2 h at 37°C in 5% CO_2. Absorbance was measured at 450 nm to determine cell viability as a percentage.

2.4. Cord Formation on Matrigel. Ninety-six-well plates were coated with 60 μL Matrigel (10 mg/mL) and allowed to polymerize at 37°C. Endothelial cells (8×10^3 cells/well) were seeded on the Matrigel and incubated at 37°C. At each time point, cells were fixed with a 4% paraformaldehyde and stained using Mayer's hematoxylin (Muto Pure Chemical, Tokyo, Japan). The cord network was photographed and cord length was measured using an Angiogenesis Image Analyzer (Kurabo, Osaka, Japan) [14].

2.5. Gene Expression Analysis by Real-Time PCR. Briefly, total RNA was extracted from cultured cells on Matrigel using TRIzol reagent (Invitrogen, Carlsbad, CA, USA). For each sample, 0.5 μg of total RNA was reverse transcribed into cDNA using the Prime Script RT reagent kit (Perfect Real Time) (TaKaRa, Dalian, China). Real-time PCR analysis was performed using the LightCycler Nano System (Roche Diagnostics, Mannheim, Germany) using FastStart Essential DNA Green Master (Roche Diagnostics) according to the manufacturer's instructions. GAPDH was used as an internal control. The relative quantification of mRNA expression was calculated as a ratio of the target gene to GAPDH. The primer sequences were as follows: HIF-1α sense, 5′-TTTTTCAAGCAGTAGGAATTGGA-3′, and antisense, 5′-GTGATGTAGTAGCTGCATGATCG-3′; VEGF-C sense, 5′-TGCCAGCAACACTACCACAG-3′, and antisense, 5′-GTGATTATTCCACATGTAATTGGT-G-3′; VEGF-A sense, 5′-CCTCCGAAACCATGAACTTT-3′, and antisense, 5′-ATGATTCTGCCCTCCTCCTT-3′; VEGF-D sense, 5′-GGAGGAAAATCCACTTGCTG-3′, and antisense, 5′-GCAACGATCTTCGTCAAAC-3′; GAPDH sense, 5′-AGCCACATCGCTCAGACAC-3′, and antisense, 5′-GCCCAATACGACCAAATCC-3′.

2.6. Detection of HIF-1α and PCNA. To determine protein levels during cord formation on Matrigel, immunoprecipitation and Western blotting were performed as described previously [14]. Cells cultured on Matrigel were washed with PBS and incubated with whole cell lysis buffer (25 mM HEPES pH 7.7, 0.3 M NaCl, 1.5 mM $MgCl_2$, 0.2 mM EDTA, 0.1% Triton X-100, 20 mM β-glycerophosphate, 1 mM sodium orthovanadate, 1 mM phenylmethylsulfonyl fluoride (PMSF), 1 mM dithiothreitol (DTT), 10 μg/mL aprotinin, and 10 μg/mL leupeptin). The cells including Matrigel were then scrubbed. The collected samples were vigorously vortexed, centrifuged at 14,000 rpm for 10 min, and the supernatant was collected. Immunoprecipitation was carried out by incubating the lysate with HIF-1α primary antibody (Santa Cruz Biotechnology) for 16 h at 4°C, followed by 12 h incubation with Dynabeads

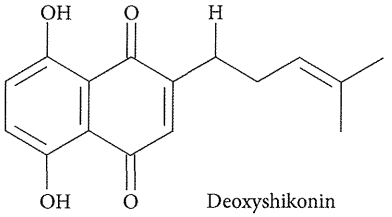

FIGURE 1: Chemical structure of deoxyshikonin.

protein G (Invitrogen). The immunoprecipitates were washed with lysis buffer, resuspended in loading buffer, boiled for 3 min, subjected to SDS-PAGE on 7.5% polyacrylamide gels, and transferred to a PVDF membrane. The primary antibody used was for HIF-1α and the secondary was polyclonal goat anti-rabbit immunoglobulin/HRP. The bands were detected using an immunochemiluminescence method. PCNA was used as the loading control.

2.7. Immunofluorescence Microscopy. Cells were seeded onto a cover slip coated with Matrigel (10 mg/mL). Cells were incubated with or without deoxyshikonin-containing medium. At the time of the experiment, the attached cells were washed with PBS, fixed with 4% paraformaldehyde (10 min), and washed and permeabilized (5 min) with 0.1% Triton X-100 in PBS. Samples were blocked with 1% BSA in PBS followed by incubation for 30 min with HIF-1α rabbit polyclonal primary antibody (Santa Cruz Biotechnology). After incubation with primary antibody, cells were washed in 0.2% Triton X-100 in PBS and then incubated with polyclonal swine anti-rabbit immunoglobulins/FITC (Dako) as a secondary antibody and Rhodamine phalloidin (Life Technologies) for 20 min. After washing, Vectashield mounting medium for DAPI staining (Vector, Burlingame, CA, USA) was added to the cells. Florescence images were captured using a Leica TCS SP5 microscope.

2.8. siRNA Transfection. Proliferating HMVEC-dLy was transfected with control siRNA or siRNA against HIF-1α (Santa Cruz Biotechnology) at a final concentration of 6 nM using Lipofectamine RNAiMAX reagents (Invitrogen). After transfection, the cells were grown for 18 h at 37°C in 5% CO_2 and trypsinized. The transfected cells combined with or without deoxyshikonin were seeded on Matrigel-coated dishes. At each time point, cells were employed for real-time PCR and cord formation assays.

2.9. Wound-Healing Assay. To investigate the potential wound-healing ability with deoxyshikonin treatment, a modified scratch assay was performed, creating gaps of precisely defined width. Culture inserts from Ibidi (Martinsried, Germany) were used in this study. This insert creates a cell-free gap (approximately 500–600 μm) [15]. Seventy microliters of cell suspension (1.8×10^5 cells/mL) were added to each well of the Ibidi culture insert. Cells were incubated at 37°C for 48 h until the cells were confluent and then the culture inserts were removed to create the gap and to allow cell migration to fill it over time. Cell migration into the gap was monitored by inverted microscopy and photographed at each time point. The distance between one side of the gap and the other can be measured by comparing the image from time 0 h to the last time point at 24 h. The distance between each gap closer was measured using Leica LAS EZ software and then calculated as the migration distance (mm).

2.10. Statistical Analysis. Statistical analysis was performed using Dunnett's method. $P < 0.05$ was considered to be significant.

3. Results

3.1. Deoxyshikonin Enhanced Cord Formation of HMVEC-dLy and HMVEC-d on Matrigel. Shikonin and some shikonin derivatives have been reported to inhibit angiogenesis [13, 16]. To find new effect of compounds that affects lymphangiogenesis and angiogenesis, deoxyshikonin was selected for use in the present study. The nontoxic dose of 0.8 μM deoxyshikonin was used to see the effect on cord formation ability of human lymphatic endothelial cells (HMVEC-dLy) and human dermal microvascular endothelial cells (HMVEC-d) (Figure 2). The cells underwent the cord formation assay and were photographed (Figures 2(a) and 2(c)) at 2 to 6 h after seeding on Matrigel. Cord length was measured by an Angiogenesis Image Analyzer and plotted as a percentage (Figures 2(b) and 2(d)). Deoxyshikonin significantly promoted cord formation ability by 64% and 28% from the control in HMVEC-dLy and HMVEC-d at 6 h of incubation, respectively (Figures 2(b) and 2(c)). This is a newly discovered effect of deoxyshikonin, which promoted to lymphangiogenesis and angiogenesis in an *in vitro* model and showed the opposite effect to shikonin (data not shown).

Because knowledge about the mechanism of lymphangiogenesis and treatment with natural compounds has not been explored sufficiently, we decided to further confirm the possible mechanism of this natural compound, deoxyshikonin, on lymphangiogenesis.

The time that showed a significant change in cord formation networks, 6 h of deoxyshikonin treatment in HMVEC-dLy, was chosen for use in further experiments.

3.2. Deoxyshikonin Dominantly Increased VEGF-C mRNA Level in HMVEC-dLy While Forming Cords on Matrigel. Endothelial cells are the target of VEGF-C, -A, and -D in lymphangiogenesis induction [4]. In addition, endothelial cells themselves can express VEGF mRNA and protein levels after stimulation [17]. The cord formation ability of HMVEC-dLy, which was enhanced by deoxyshikonin (Figures 2(a) and 2(b)), may occur as a result of the increase of VEGFs.

We further examined the effect of deoxyshikonin on the expression of VEGF-C, VEGF-A, and VEGF-D mRNA during cord formation of HMVEC-dLy. Real-time PCR was used to determine transcription levels of these genes.

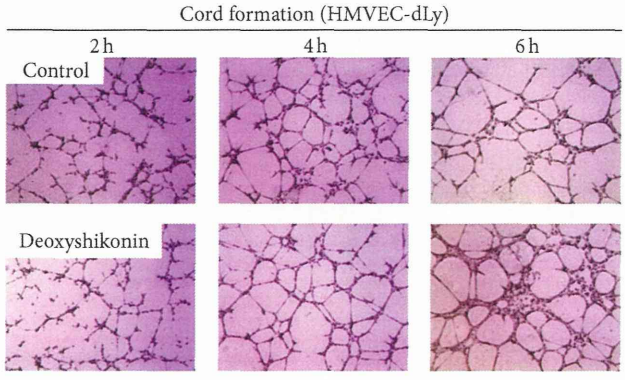

(a)

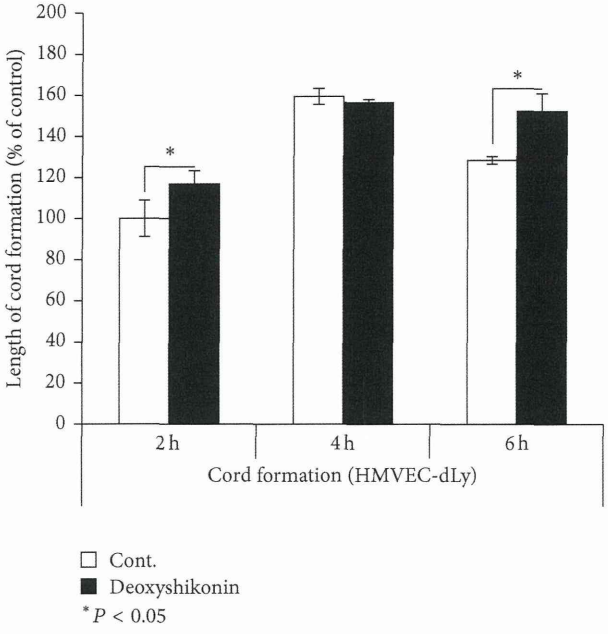

(b)

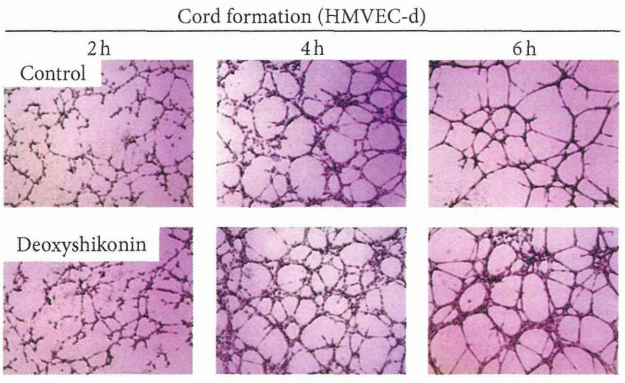

(c)

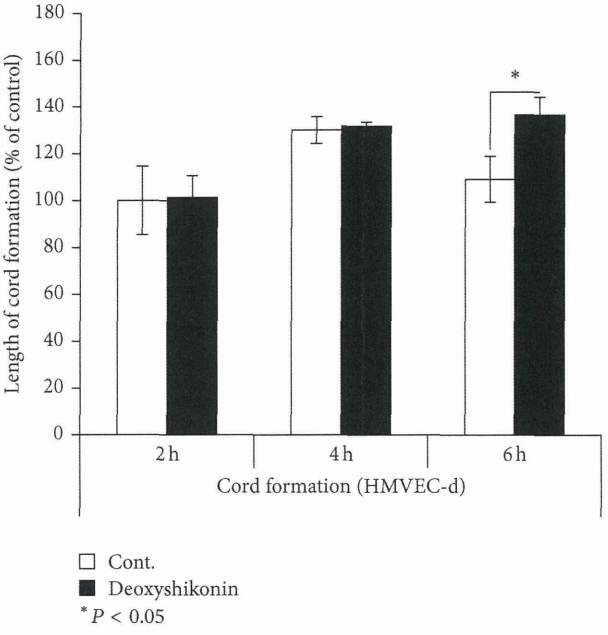

(d)

FIGURE 2: Effects of deoxyshikonin on cord formation of HMVEC-dLy and HMVEC-d on Matrigel. (a), (c) Photographs of cord formation of HMVEC-dLy and HMVEC-d on Matrigel after incubation with or without 0.8 μM deoxyshikonin at 2 to 6 h (at ×400 magnification). (b), (d) The relative length of cords was measured using an Angiogenesis Image Analyzer. Data are the mean ± SD ($n = 3$); $^{*}P < 0.05$, $^{**}P < 0.01$ compared with the control.

Endothelial cells were seeded on Matrigel and incubated with 0.8 μM deoxyshikonin for 6 h. The mRNA was collected and subjected to real-time PCR (Figure 3(b)). The cord formation assay was also performed for comparison at the same time of incubation (Figure 3(a)). The results showed that deoxyshikonin significantly increased mRNA expression levels of VEGF-C and VEGF-A in HMVEC-dLy by 0.42-fold and 0.32-fold when compared with their control, respectively (Figure 3(b)). These increases also correlated with the increase of cord formation of endothelial cells at the same time of treatment (Figure 3(a)); however, VEGF-D mRNA levels were expressed at very low levels (Figure 3(b)). This indicated that deoxyshikonin-induced cord formation networks in HMVEC-dLy were involved in the induction of

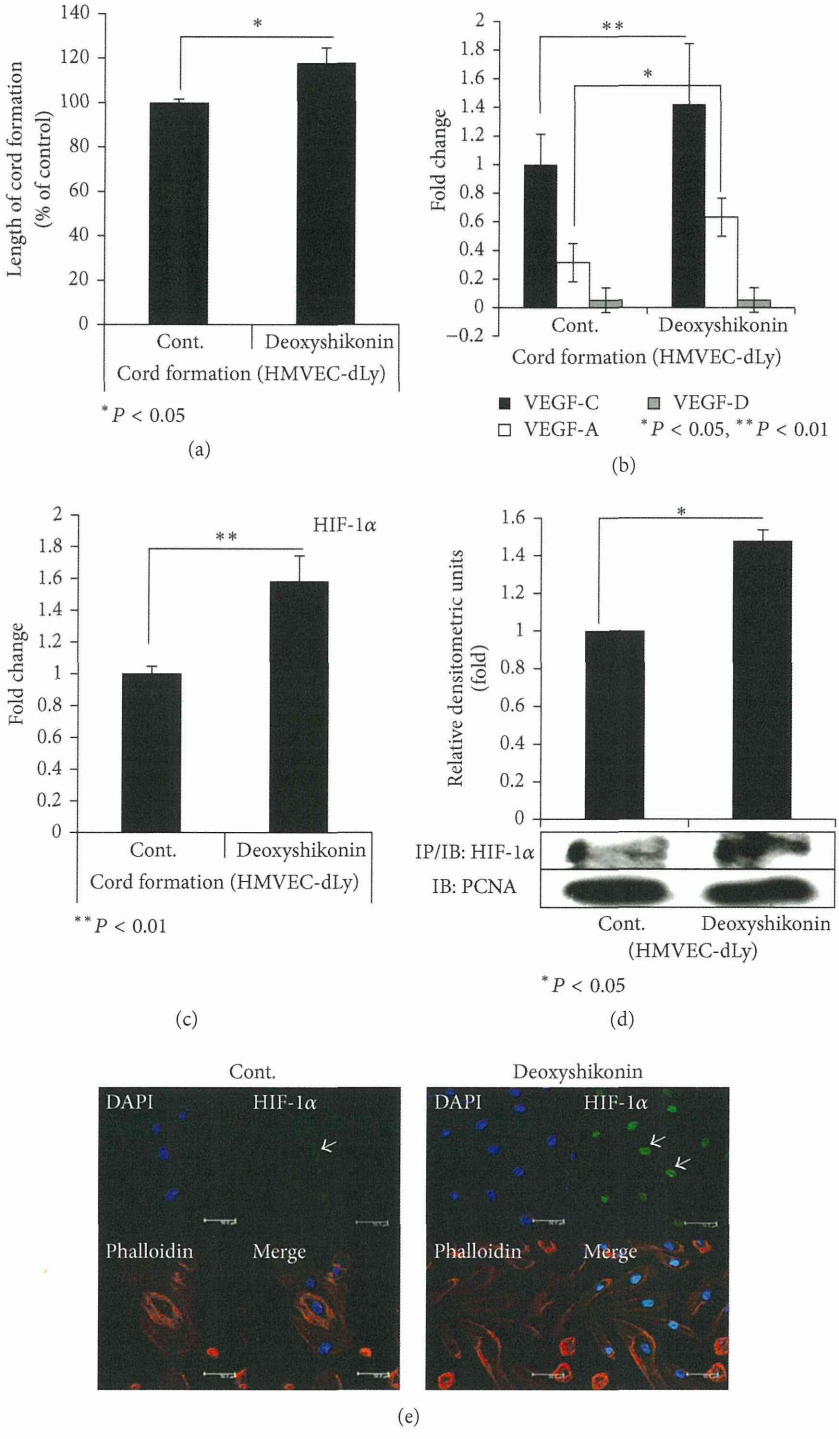

FIGURE 3: Effect of deoxyshikonin on VEGF-C, -A, and -D mRNA levels and regulation of HIF-1α during cord formation of HMVEC-dLy on Matrigel. Cells were exposed with or without 0.8 μM deoxyshikonin for 6 h and then underwent experiments. (a) The relative length of cords was measured using an Angiogenesis Image Analyzer. (b), (c) VEGF-C, -A, and -D and also HIF-1α mRNA levels were detected by real-time PCR. (d) The HIF-1α protein level was determined by immunoprecipitation and Western blotting. The results were analyzed by scanning and Scion Image software. (e) HIF-1α nuclear translocation as determined by immunofluorescence microscopy. Similar results were obtained in three independent experiments; $^{*}P < 0.05$, $^{**}P < 0.01$ compared with their control.

VEGF-C and VEGF-A mRNA levels, which had a greater potential effect on the increase of the VEGF-C mRNA level than the VEGF-A mRNA level (Figure 3(b)).

VEGF-C is the main vascular endothelial growth factor important for lymphangiogenesis [18, 19]. As the next step, we studied the possible mechanisms of deoxyshikonin induction in lymphangiogenesis *in vitro* by using HMVEC-dLy.

3.3. Deoxyshikonin Regulates HIF-1α at Transcriptional, Post-transcriptional, and Functional Levels in HMVEC-dLy during Cord Formation on Matrigel. HIF-1α plays a certain role in lymphangiogenesis by closely correlating with lymphatic expression of VEGF-C in cancers, wound healing, and inflammation [7, 20, 21], and we found that deoxyshikonin upregulated the VEGF-C mRNA level during lymphangiogenesis *in vitro* (Figure 3(b)). In addition, the function of HIF-1 can be regulated by several stimuli under normoxic conditions [4, 5]. Deoxyshikonin, which promoted cord formation of HMVEC-dLy in this study, may correlate with VEGF-C mRNA expression and HIF-1α regulation.

To determine the effect of deoxyshikonin on HIF-1α regulation, real-time PCR, immunoprecipitation/Western blotting, and immunofluorescence microscopy were performed to see the expression of HIF-1α mRNA, HIF-1α protein, and also the activation of HIF-1α, respectively. HMVEC-dLy were seeded on Matrigel, cultured with or without 0.8 μM deoxyshikonin-containing medium, and left to form cord networks for 6 h. Then, mRNA and protein were collected to measure mRNA and protein expression levels. Figure 3(c) shows that the HIF-1α mRNA level was increased 0.58-fold that of the control (Figure 3(c)) and the HIF-1α protein level also significantly increased after deoxyshikonin treatment (Figure 3(d)). The nuclear translocation of HIF-1α was also determined (Figure 3(e)). Cells were seeded on Matrigel-coated slides and then treated with or without 0.8 μM deoxyshikonin for 6 h. Immunofluorescence microscopy was performed and photographed (Figure 3(e)). HIF-1α is a cytoplasmic protein. During activation, HIF-1α will dimerize with HIF-1β and then translocate to the nucleus to give the active transcription factor of HIF-1. In our results, HMVEC-dLy treated with deoxyshikonin showed the accumulation of HIF-1α inside the nucleus, which indicated the activation of HIF-1α transcription factor. These results conclude that deoxyshikonin induced cord formation of HMVEC-dLy and was involved in the regulation of HIF-1α at the transcriptional, posttranscriptional, and functional levels.

3.4. Deoxyshikonin-Induced VEGF-C mRNA Expression and Cord Formation of HMVEC-dLy via HIF-1α Regulation. To see whether HIF-1α controls VEGF-C mRNA expression during cord formation of deoxyshikonin-treated cells, siHIF-1α transfection was used in this study. siCont- and siHIF-1α-transfected cells were seeded on Matrigel and incubated with or without 0.8 μM deoxyshikonin for 2–6 h. At each time point, cells underwent a cord formation assay (Figure 4(c)) and mRNA was collected to perform real-time PCR (Figures 4(a) and 4(b)). The results showed that HMVEC-dLy, which was transfected with siHIF-1α, successfully suppressed HIF-1α mRNA expression throughout the experiment (Figure 4(a)). During incubation, in the absence of deoxyshikonin, VEGF-C mRNA expression was significantly decreased in HIF-1α knockdown cells, by 0.25-fold, 0.5-fold, and 0.2-fold at 2, 4, and 6 h, respectively (Figure 4(b)) and these decreases also correlated with the significant decrease in the length of cord formation by the HIF-1α knockdown cells, by 38%, 56%, and 46% at 2, 4, and 6 h, respectively, (Figure 4(c)). These results indicated that HIF-1α controlled VEGF-C mRNA expression and cord formation ability in HMVED-dLy. In addition, deoxyshikonin treatment in siCont-transfected cells significantly increased HIF-1α and VEGF-C mRNA expression at 6 h (Figures 4(a) and 4(b)) when compared with their control groups. These increases also correlated with the significantly increased cord formation at the same incubation time (6 h) (Figure 4(c)). Interestingly, deoxyshikonin treatment of HIF-1α knockdown cells did not restore VEGF-C mRNA expression (Figure 4(b)) and cord formation (Figure 4(c)) to the control levels but only slightly increased their levels when compared to untreated HIF-1α knockdown cells.

These results indicated that deoxyshikonin promoted VEGF-C mRNA expression and the cord formation ability of HMVEC-dLy, mainly via HIF-1α-dependent regulation.

3.5. Deoxyshikonin Promoted Wound Healing In Vitro. We therefore succeeded in proving the mechanism of deoxyshikonin on the cord formation of HMVEC-dLy, which was involved in the regulation of HIF-1α and VEGF-C mRNA expression. As the next step, we assessed the potential of deoxyshikonin-induced lymphangiogenesis for clinical applications such as wound-healing treatment, because the promotion of lymphangiogenesis can improve wound-healing [22]. We performed a wound healing assay using culture inserts from Ibidi to create a cell-free gap and measured the gap distance (migration distance) using Leica LAS EZ software. The result showed that incubating the cells with 0.8 μM deoxyshikonin promoted the migration of HMVEC-dLy by significantly inducing cell filling of the gap when compared to the control at 24 h of incubation (Figures 5(a) and 5(b)). Some of the effect of deoxyshikonin on apparent cell migration might be a contribution from cell proliferation. The proliferation assay (Figure 5(c)) confirmed that at a deoxyshikonin concentration of 0.8 μM, the cells filling the gap of the wound did not arise from cell proliferation. However, at higher concentrations (1.6 and 3 μM), deoxyshikonin significantly induced proliferation of HMVEC-dLy. This result indicated that deoxyshikonin could be used to improve wound healing by inducting lymphatic endothelial cell migration and lymphangiogenesis.

4. Discussion

In this study, we used primary endothelial cells, human dermal lymphatic microvascular endothelial cells (HMVEC-dLy), to investigate a new effect of deoxyshikonin (Figure 1), on lymphangiogenesis *in vitro* by comparing them with

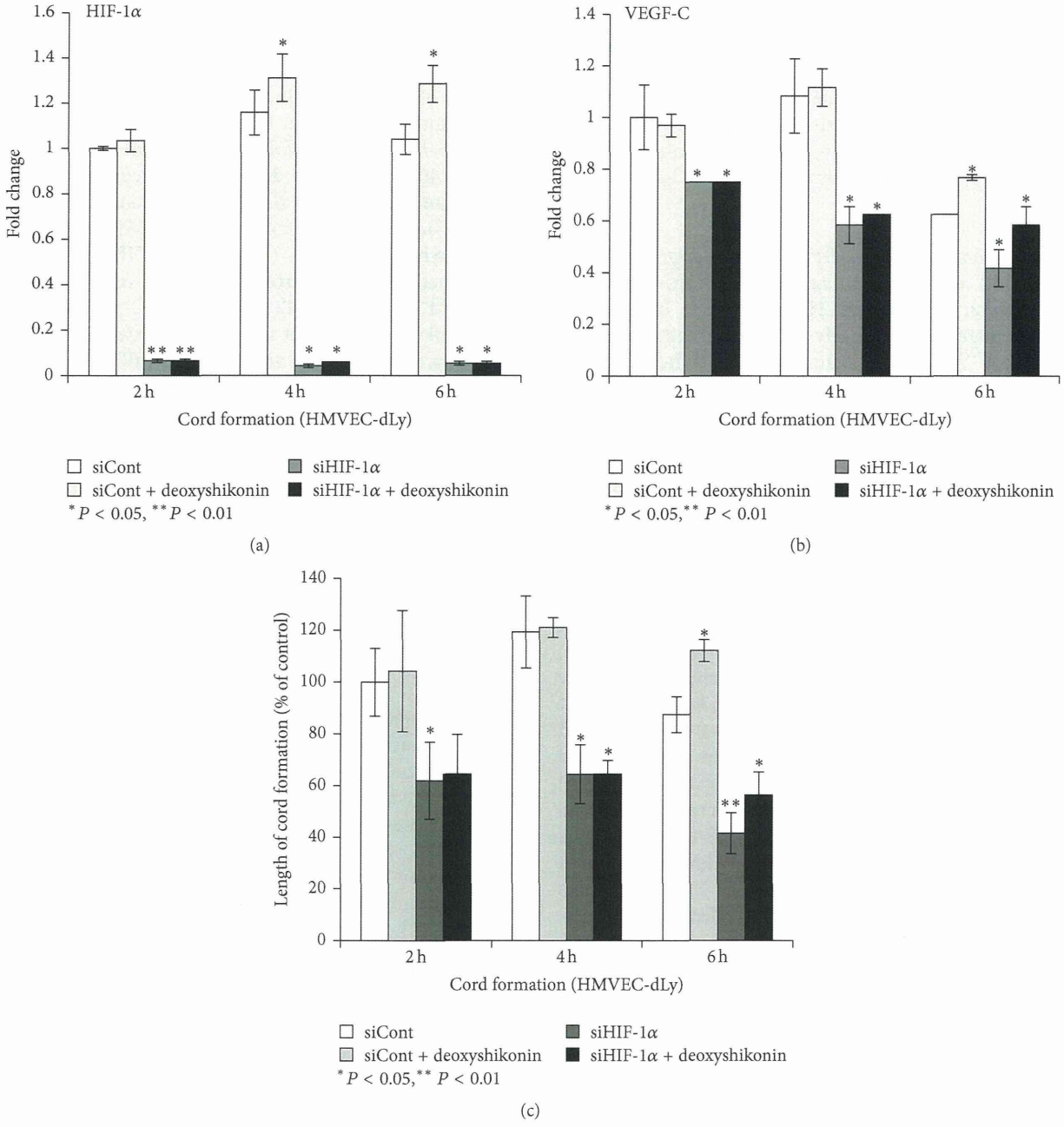

FIGURE 4: Deoxyshikonin regulates VEGF-C mRNA levels and cord formation of HMVEC-dLy via HIF-1α. After transfection with control siRNA or siRNA for HIF-1α, HMVEC-dLy cells were seeded on Matrigel and incubated with or without 0.8 μM deoxyshikonin for 2–6 h, and then cells were subjected to real-time PCR and cord formation assay. (a) HIF-1α mRNA levels. (b) VEGF-C mRNA levels. (c) Relative length of cord formations. Similar results were obtained in three independent experiments; $^{*}P < 0.05$, $^{**}P < 0.01$ compared with the control.

human dermal microvascular endothelial cells (HMVEC-d). We continued to explore the possible mechanism by investigating the expression of important genes involved in cord formation networks of lymphatic endothelial cells after treatment with deoxyshikonin.

Previous reports found that deoxyshikonin has antifungal [23] and antitumor activities [24, 25], but there was no evidence of a lymphangiogenesis or angiogenesis effect. Shikonin and some derivative forms such as acetylshikonin, isobutyroylshikonin, and β-hydroxyisovalerylshikonin are already known to have an antiangiogenesis effect on an *in vivo* and *in vitro* model and the controlling molecules are known [9, 13, 16]; however, the effect of shikonin and its derivatives, including deoxyshikonin, on lymphangiogenesis has not been discovered.

The nontoxic dose of deoxyshikonin was confirmed (Figure 5(c)) and selected in a proliferation assay before performing the experiments. Our results show for the

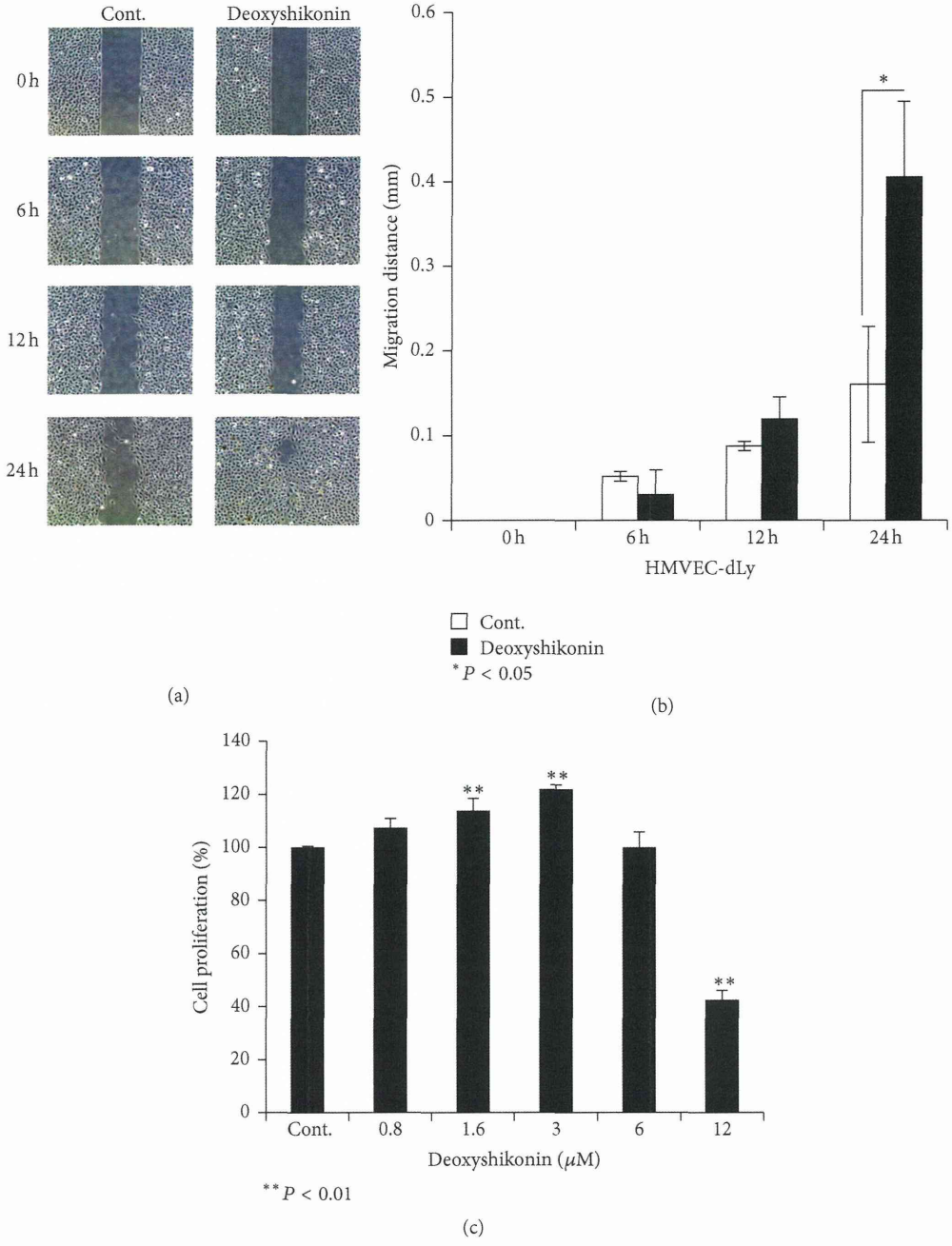

FIGURE 5: Deoxyshikonin promoted wound healing *in vitro* by inducing the HMVEC-dLy migration ability. After growing the HMVEC-dLy in culture inserts that create a cell-free gap, migration of cells to fill the gap was monitored at regular intervals. (a) Photograph of cell migration into the gap from 0 to 24 h in deoxyshikonin treatment and control group. (b) The migration ability of the cells was measured using Leica LAS EZ software and the migration distances calculated (mm). (c) The effects of deoxyshikonin on cell proliferation were determined by a proliferation assay and the data are plotted as percentages of control cell proliferation. Data are the mean ± SD ($n = 3$); $^{*}P < 0.05$, $^{**}P < 0.01$ compared with the control.

first time that deoxyshikonin has a potential to promote lymphangiogenesis and angiogenesis in an *in vitro* model, which interestingly showed opposite effects with shikonin (See Supplementary Figures 1(b) and 1(c) available online at http://dx.doi.org/10.1155/2013/148297). We showed for the first time that deoxyshikonin has a prolymphangiogenesis (Figures 2(a) and 2(b)) as well as a proangiogenesis effect *in vitro* (Figures 2(c) and 2(d)).

The processes of the cord formation of endothelial cells after seeding on Matrigel, which mimics the extracellular matrix [26], include the promotion of cell adhesion, survival, and migration, including cell proliferation for sprouting

and finding each other and maintaining the formation cord networks [27], and VEGFs such as VEGF-C, VEGF-A, and VEGF-D are widely known to induce lymphangiogenesis and angiogenesis *in vitro* and *in vivo* by enhancing these processes [28]. Generally, endothelial cells are the target, not the main source of VEGFs; however, it has been also demonstrated that human dermal microvascular endothelial cells themselves can express mRNA and release an amount of these growth factors [17, 28]. We found that deoxyshikonin significantly increased the expression of VEGF-C mRNA and VEGF-A mRNA in HMVEC-dLy but had no effect on VEGF-D (Figure 3(b)). The increase of VEGF-C and VEGF-A correlated with the significant induction of the cord formation of HMVEC-dLy at the time of deoxyshikonin treatment (Figure 3(a)). Endothelium-derived VEGF can induce neovascularization through proliferation, and increase the migration of dermal microvascular cells [29]. The increase of VEGF-C and VEGF-A mRNA expression after deoxyshikonin treatment could proceed to protein products, be secreted, and then interact with specific membrane receptors of endothelial cells displaying tyrosine kinase activity [17]. Binding of VEGF-A with VEGFR-2 and binding of VEGF-C with VEGFR-2 and VEGFR-3 promote the cord formation of HMVEC-dLy on Matrigel (Figure 3(a)). Interestingly, the results (Figure 3(b)) show that the mRNA levels of VEGF-C after deoxyshikonin treatment were high when compared with VEGF-A. As VEGF-C acts as a key growth factor in physiological lymphangiogenesis and was found to promote the activation of VEGF-3, a specific receptor expressed in lymphatic endothelium [18, 19], we focused our study on the mechanism of deoxyshikonin on lymphangiogenesis *in vitro*.

HIF-1 is an oxygen-regulated transcriptional factor that plays a role in tumor lymphangiogenesis, wound healing and inflammation by regulating the lymphatic expression of VEGF-C [7, 20, 21]. In addition, HIF-1-mediated pathways also promote or repress the transcription of a broad range of genes that are involved in maintaining biological homeostasis, such as influencing metabolic adaptation, the innate immune response, cell survival, and apoptosis [4, 5]. In hypoxia, HIF-1α protein persists and the HIF-1α/β complex stimulates VEGF release in almost all cell types. Under normoxia, HIF-1α protein is subjected to ubiquitin-dependent degradation [4]; however, HIF-1α is also expressed and functions in response to stimulation by several growth factors by the mechanism different from the hypoxic condition [5].

In this study, we performed experiments under normoxic conditions. For the first time we found that deoxyshikonin regulated HIF-1α at transcriptional, posttranscriptional, and functional levels (Figures 3(c), 3(d), and 3(e)) during cord formation of HMVEC-dLy (Figure 3(a)). Similar recent reports mentioned that several nonhypoxic effectors and signaling pathways have been proven to enhance HIF-1α levels through the activation of regulative mechanisms distinct from protein stabilization. Some of these stimuli also regulate HIF-1α at the transcriptional, posttranscriptional, or translational level or additionally influence posttranslational modifications, including the functions of HIF-1α protein [4, 5]. For example, lipopolysaccharides (LPS) and cytokines activate the nuclear factor-κB (NF-κB) signaling pathway promoting HIF-1α transcription [30], whereas some growth factors such as epithelial growth factors (EGF), fibroblast growth factor 2 (FGF2), and insulin-like growth factor (IGF) enhance the translation of HIF-1α protein [31]. In addition, loss of function of tumor suppressors (such as p53, PTEN, and VHL) and gain of function of oncogenes (such as AKT, MYC, mTOR, PI3 K, RAF, and RAS) also regulate different steps that lead to the activation of HIF function [31, 32].

Deoxyshikonin might contribute to the signaling pathways mentioned above, enhance HIF-1α mRNA/protein expression and activate nuclear translocation (Figures 3(c), 3(d), and 3(e)); however, we did not prove the effect of deoxyshikonin on the signal transduction pathway in this study. Once in the nucleus, deoxyshikonin could promote HIF-1α and HIF-1β subunit interaction and bind to specific DNA sequences targeted by HIF, known as hypoxia response elements (HREs), which are composed of 5′-RCGTG-3′, leading to the stimulation of VEGF release, especially VEGF-C, which induced cord formation of HMVEC-dLy (Figures 3(a) and 3(b)). Successful suppression of the HIF-1α gene using siRNA transfection confirmed that HIF-1α regulated VEGF-C mRNA expression and the cord formation ability of HMVEC-dLy on Matrigel (Figure 4).

Although VEGF mRNA, including VEGF-C mRNA expression, can be upregulated by HIF-1, several transcription factors such as AP-1, Sp-1, and NF-κB also induce VEGF expression by binding to the promoter to initiate and activate the transcription of the VEGF gene directly [6]. We also proved this by using deoxyshikonin treatment in HIF-1α knockdown cells and found that deoxyshikonin could not recover VEGF-C mRNA expression and the cord formation of HMVEC-dLy back to the control level but only slightly increased when compared with HIF-1α knockdown cells alone (Figure 4). This result indicated that deoxyshikonin induced VEGF-C mRNA expression and the cord formation of HMVEC-dLy, mainly via HIF-1α-dependent regulation, and may also contribute to HIF-1α-independent regulation; however, the details of these mechanisms still need to be further investigated.

The promotion of lymphatic vessel generation improved wound function to maintain normal tissue pressure by draining protein-rich lymph from the interstitial space and facilitate the delivery of cells that mediate the immune response [22]. In this study we proved that deoxyshikonin promoted lymphangiogenesis (Figure 2) and also wound healing *in vitro* by facilitating the migration of HMVEC-dLy into the wound gap (Figure 5), which indicated that deoxyshikonin could be developed for use in wound-healing treatment. However, wound healing is a complicated biological process as it involves the interactions of multiple cell types, various cytokines, growth factors, their mediators, and extracellular matrix proteins [11], and the details of deoxyshikonin in wound healing require further proof *in vitro* and also *in vivo*.

In conclusion, we discovered a new effect of deoxyshikonin, which is included in shiunko as a typical Kampo drug ointment used for the treatment of wound healing in Japan, that enhanced cord formation of HMVEC-dLy via HIF-1α-controlled VEGF-C mRNA regulation and also promoted

wound healing in an *in vitro* model. This finding may offer new therapeutic options for using deoxyshikonin compounds that modulate HIF-1α and VEGF-C under nonhypoxic conditions in wound healing and other lymphatic diseases.

Conflict of Interests

The authors declare that they have no conflict of interests.

Acknowledgment

This study was supported by a Grant-in-Aid for Scientific Research (C) (no. 22501042).

References

[1] T. Tammela and K. Alitalo, "Lymphangiogenesis: molecular mechanisms and future promise," *Cell*, vol. 140, no. 4, pp. 460–476, 2010.

[2] L. N. Cueni and M. Detmar, "The lymphatic system in health and disease," *Lymphatic Research and Biology*, vol. 6, no. 3-4, pp. 109–122, 2008.

[3] R. Roskoski Jr., "Vascular endothelial growth factor (VEGF) signaling in tumor progression," *Critical Reviews in Oncology/Hematology*, vol. 62, no. 3, pp. 179–213, 2007.

[4] M. C. Brahimi-Horn and J. Pouysségur, "HIF at a glance," *Journal of Cell Science*, vol. 122, no. 8, pp. 1055–1057, 2009.

[5] A. Kuschel, P. Simon, and S. Tug, "Functional regulation of HIF-1α under normoxia—is there more than post-translational regulation?" *Journal of Cellular Physiology*, vol. 227, no. 2, pp. 514–524, 2012.

[6] J. Jośko and M. Mazurek, "Transcription factors having impact on vascular endothelial growth factor (VEGF) gene expression in angiogenesis," *Medical Science Monitor*, vol. 10, no. 4, pp. RA89–RA98, 2004.

[7] J. C. Zampell, A. Yan, T. Avraham, S. Daluvoy, E. S. Weitman, and B. J. Mehrara, "HIF-1α coordinates lymphangiogenesis during wound healing and in response to inflammation," *The FASEB Journal*, vol. 26, no. 3, pp. 1027–1039, 2012.

[8] J. P. Bridges, S. Lin, M. Ikegami, and J. M. Shannon, "Conditional hypoxia inducible factor-1α induction in embryonic pulmonary epithelium impairs maturation and augments lymphangiogenesis," *Developmental Biology*, vol. 362, no. 1, pp. 24–41, 2012.

[9] T. Hisa, Y. Kimura, K. Takada, F. Suzuki, and M. Takigawa, "Shikonin, an ingredient of *Lithospermum erythrorhizon*, inhibits angiogenesis *in vivo* and *in vitro*," *Anticancer Research*, vol. 18, no. 2A, pp. 783–790, 1998.

[10] P. J. Lu, C. Yang, C. N. Lin et al., "Shiunko and acetylshikonin promote reepithelialization, angiogenesis, and granulation tissue formation in wounded skin," *American Journal of Chinese Medicine*, vol. 36, no. 1, pp. 115–123, 2008.

[11] G. C. Gurtner, S. Werner, Y. Barrandon, and M. T. Longaker, "Wound repair and regeneration," *Nature*, vol. 453, no. 7193, pp. 314–321, 2008.

[12] X. Chen, L. Yang, J. J. Oppenheim, and O. M. Z. Howard, "Cellular pharmacology studies of shikonin derivatives," *Phytotherapy Research*, vol. 16, no. 3, pp. 199–209, 2002.

[13] H. J. Lee, H. J. Lee, V. Magesh et al., "Shikonin, acetylshikonin, and isobutyroylshikonin inhibit VEGF-induced angiogenesis and suppress tumor growth in Lewis lung carcinoma-bearing mice," *Yakugaku Zasshi*, vol. 128, no. 11, pp. 1681–1688, 2008.

[14] O. Prangsaengtong, K. Koizumi, K. Senda, H. Sakurai, and I. Saiki, "ENOS and Hsp90 interaction directly correlates with cord formation in human lymphatic endothelial cells," *Lymphatic Research and Biology*, vol. 9, no. 1, pp. 53–59, 2011.

[15] N. Andrae, E. Kirches, R. Hartig et al., "Sunitinib targets PDGF-receptor and Flt3 and reduces survival and migration of human meningioma cells," *European Journal of Cancer*, vol. 48, no. 12, pp. 1831–1841, 2012.

[16] Y. Komi, Y. Suzuki, M. Shimamura et al., "Mechanism of inhibition of tumor angiogenesis by β-hydroxyisovalerylshikonin," *Cancer Science*, vol. 100, no. 2, pp. 269–277, 2009.

[17] B. Vega-Diaz, G. S. Herron, and S. Michel, "An autocrine loop mediates expression of vascular endothelial growth factor in human dermal microvascular endothelial cells," *Journal of Investigative Dermatology*, vol. 116, no. 4, pp. 525–530, 2001.

[18] M. J. Karkkainen, P. Haiko, K. Sainio et al., "Vascular endothelial growth factor C is required for sprouting of the first lymphatic vessels from embryonic veins," *Nature Immunology*, vol. 5, no. 1, pp. 74–80, 2004.

[19] S. J. Mandriota, L. Jussila, M. Jeltsch et al., "Vascular endothelial growth factor-C-mediated lymphangiogenesis promotes tumour metastasis," *The EMBO Journal*, vol. 20, no. 4, pp. 672–682, 2001.

[20] S. F. Schoppmann, A. Fenzl, M. Schindl et al., "Hypoxia inducible factor-1α correlates with VEGF-C expression and lymphangiogenesis in breast cancer," *Breast Cancer Research and Treatment*, vol. 99, no. 2, pp. 135–141, 2006.

[21] X. Liang, D. Yang, J. Hu, X. Hao, J. Gao, and Z. Mao, "Hypoxia inducible factor-1alpha expression correlates with vascular endothelial growth factor-C expression and lymphangiogenesis/angiogenesis in oral squamous cell carcinoma," *Anticancer Research*, vol. 28, no. 3A, pp. 1659–1666, 2008.

[22] K. Maruyama, J. Asai, M. Ii, T. Thorne, D. W. Losordo, and P. A. D'Amore, "Decreased macrophage number and activation lead to reduced lymphatic vessel formation and contribute to impaired diabetic wound healing," *American Journal of Pathology*, vol. 170, no. 4, pp. 1178–1191, 2007.

[23] K. Sasaki, H. Abe, and F. Yoshizaki, "*In vitro* antifungal activity of naphthoquinone derivatives," *Biological and Pharmaceutical Bulletin*, vol. 25, no. 5, pp. 669–670, 2002.

[24] S. Rajasekar, D. J. Park, C. Park et al., "*In vitro* and *in vivo* anticancer effects of Lithospermum erythrorhizon extract on B16F10 murine melanoma," *Journal of Ethnopharmacology*, vol. 144, no. 2, pp. 335–345, 2012.

[25] Y. Xuan and X. Hu, "Naturally-occurring shikonin analogues—a class of necroptotic inducers that circumvent cancer drug resistance," *Cancer Letters*, vol. 274, no. 2, pp. 233–242, 2009.

[26] H. K. Kleinman and G. R. Martin, "Matrigel: basement membrane matrix with biological activity," *Seminars in Cancer Biology*, vol. 15, no. 5, pp. 378–386, 2005.

[27] D. H. Ausprunk and J. Folkman, "Migration and proliferation of endothelial cells in preformed and newly formed blood vessels during tumor angiogenesis," *Microvascular Research*, vol. 14, no. 1, pp. 53–65, 1977.

[28] S. Dias, M. Choy, K. Alitalo, and S. Rafii, "Vascular endothelial growth factor (VEGF)-C signaling through FLT-4 (VEGFR-3) mediates leukemic cell proliferation, survival, and resistance to chemotherapy," *Blood*, vol. 99, no. 6, pp. 2179–2184, 2002.

[29] M. Detmar, "Molecular regulation of angiogenesis in the skin," *Journal of Investigative Dermatology*, vol. 106, no. 2, pp. 207–208, 1996.

[30] A. Görlach and S. Bonello, "The cross-talk between NF-kappaB and HIF-1: further evidence for a significant liaison," *The Biochemical Journal*, vol. 412, no. 3, pp. e17–e19, 2008.

[31] G. L. Semenza, M. K. Nejfelt, S. M. Chi, and S. E. Antonarakis, "Hypoxia-inducible nuclear factors bind to an enhancer element located 3' to the human erythropoietin gene," *Proceedings of the National Academy of Sciences of the United States of America*, vol. 88, no. 13, pp. 5680–5684, 1991.

[32] C. V. Dang, J. W. Kim, P. Gao, and J. Yustein, "The interplay between MYC and HIF in cancer," *Nature Reviews Cancer*, vol. 8, no. 1, pp. 51–56, 2008.

Bioorganic & Medicinal Chemistry Letters 22 (2012) 3001–3005

Contents lists available at SciVerse ScienceDirect

Bioorganic & Medicinal Chemistry Letters

journal homepage: www.elsevier.com/locate/bmcl

Synthesis and evaluation of 1-(substituted)-3-prop-2-ynylureas as antiangiogenic agents

Kingkan Sanphanya [a], Suvara K. Wattanapitayakul [b], Orawin Prangsaengtong [c], Michiko Jo [c], Keiichi Koizumi [c], Naotoshi Shibahara [c], Aroonsri Priprem [d], Valery V. Fokin [e], Opa Vajragupta [a,*]

[a] Department of Pharmaceutical Chemistry, Faculty of Pharmacy, Mahidol University, 447 Sri-Ayudya Rd, Bangkok 10400, Thailand
[b] Department of Pharmacology, Faculty of Medicine, Srinakharinwirot University, 114 Sukhumvit 23, Bangkok 10110, Thailand
[c] Department of Kampo Diagnostics, Institute of Natural Medicine, University of Toyama, 2630 Sugitani, Toyama-shi, Toyama 930-0194, Japan
[d] Department of Pharmaceutical Technology, Faculty of Pharmaceutical Sciences, Khon Kaen University, Khon Kae 40002, Thailand
[e] Department of Chemistry, The Scripps Research Institute, 10550 North Torrey Pines Rd, La Jolla, CA 92037, USA

ARTICLE INFO

Article history:
Received 12 September 2011
Revised 20 January 2012
Accepted 10 February 2012
Available online 22 February 2012

Keywords:
1-(Substituted)-3-prop-2-ynylurea
Cytotoxic agents
Tyrosine kinase inhibitors
EGFR kinase inhibitor
Antiangiogenic agent

ABSTRACT

Novel urea derivatives of alkynes have been designed, synthesized, and evaluated as potential cancer therapeutics leads. The most active 1-((3-chloromethyl)phenyl)-3-prop-2-ynylurea (**1**) exhibited cytotoxic effect against HELA and MCF-7 cell lines with IC_{50} values of 1.55 μM and 1.48 μM, respectively. Further investigation on tube formation assay in human vein umbilical cells (HUVEC) demonstrated that **1** and methyl 4-(3-(3-ethynylureido)benzyloxy) benzoate (**6**) possess antiangiogenic activity, with minimum effective dose of 25 nM (for **1**) and 6.25 μM (for **6**). The ED_{50} of **1** and **6** were found to be 0.26 μM and 17.52 μM, respectively. The results from in vitro tyrosine kinase assay indicated the EGFR inhibition of **1** over other kinases (VEGFR2, FGFR1 and PDGFRβ). The cytotoxicity of **1** against EGFR overexpressing cell line A431 (IC_{50} 36 nM) was comparable to that of erlotinib. The binding mode of **1** from docking simulation in the EGFR active site revealed that the urea motif formed hydrogen bonding with Lys745, Thr854 and Asp855 in hydrophobic pocket of EGFR. Compound **1** is considered as a potential lead for further optimization.

Protein tyrosine kinases (TKs), a family of cell signaling proteins that regulate inter- and intracellular communications, have been implicated in cancer development. Two classes of TKs, categorized by structures, functions and locations, are receptor tyrosine kinases (RTKs) and non-receptor tyrosine kinases (NRTKs). These TKs play an important role in regulation of cell growth, proliferation, differentiation, survival and metabolism.[1,2] RTKs such as vascular endothelial growth factor receptor-2 (VEGFR2), epidermal growth factor receptor (EGFR), fibroblast growth factor receptor-1 (FGFR1), and platelet-derived growth factor receptor (PDGFR) play a key role in angiogenesis, the sprouting process of capillaries from pre-existing vessels. These RTKs are important targets in antiangiogenic drug development. Inhibition of these enzymes can lead to suppression of both cell proliferation and angiogenesis and may become a viable strategy in cancer treatment.[3]

Urea derivatives demonstrate diverse array of biological and pharmacological activities, such as antibacterial, antifungal, anti-inflammatory, antiangiogenic and antiproliferative properties.[4–6] Sorafenib is an example of an anti-proliferative urea agent (Fig. 1).[7–9] It is a tyrosine kinase inhibitor (VEGFR and PDGFR) which was approved by the US FDA for advanced renal cancer.[10]

The 1-(substituted)-3-prop-2-ynylureas, terminal alkynes bearing urea motif, were firstly designed in our lab as an in-house library for the preparation of 1,4-disubsituted-1,2,3-triazole derivatives by copper-catalyzed azide alkyne cycloaddition (CuAAC) reaction.[11]

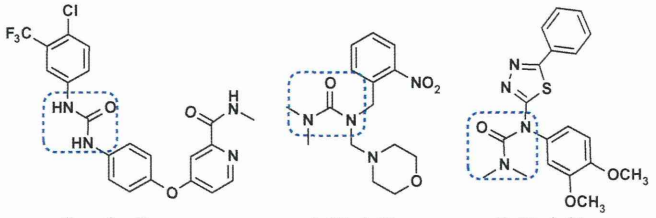

Sorafenib
IC_{50}(MDA-MB-231) = 2.5 μM

A [Ref. 8]
IC_{50} (KB) = 2.5 μM
IC_{50} (K562) = 0.4 μM

B [Ref. 9]
IC_{50} (K562) = 3 μM

Figure 1. Substituted ureas acting as antiproliferative agents. MDA-MB-231, KB and K562 are human breast cancer cell line, human carcinoma of the nosopharynx and human erythroleukemia cell line, respectively.

* Corresponding author. Tel.: +66 26 448 677; fax: +66 26 448 695.
E-mail address: pyovj@mahidol.ac.th (O. Vajragupta).

0960-894X/$ - see front matter © 2012 Elsevier Ltd. All rights reserved.
doi:10.1016/j.bmcl.2012.02.029

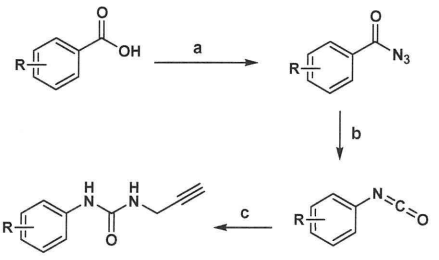

Scheme 1. General synthesis of urea compounds **1–5**. Reagents and conditions: (a) DPPA, TEA, toluene or dioxane, rt, 30 min; (b) toluene or dioxane, 100 °C, 1 h; (c) propargylamine, rt, 30 min.

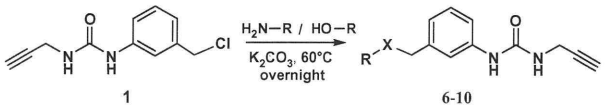

Scheme 2. General synthesis of urea compounds **6–10**.

Table 1
Yields and melting points of the synthesized 1-(substituted)-3-prop-2ynylureas

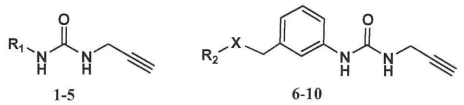

Compoundd	R_1	X	R_2	% Yield	Mp (°C)
1	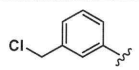	–	–	21.48	158–160
2	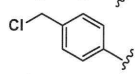	–	–	10.01	132–134
3	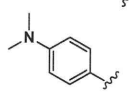	–	–	50.27	178–180
4		–	–	72.48	122–124
5	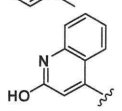	–	–	10.53	246–248
6	–	O	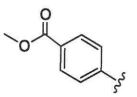	38.12	179–181
7	–	NH	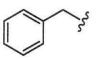	12.23	68–72
8	–	NH	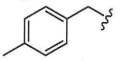	25.53	119–120
9	–	NH	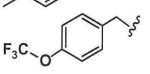	15.34	112–114
10	–	NH	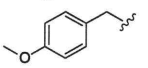	34.87	99–101

The synthesized triazole-based ureas, as well as the azide and alkyne precursors, were screened for their cytotoxic effects against HELA and MCF-7 cell lines. 1-(3-Chloromethyl)-3-prop-2-ynylurea **1** showed cytotoxic effect against HELA and MCF-7.

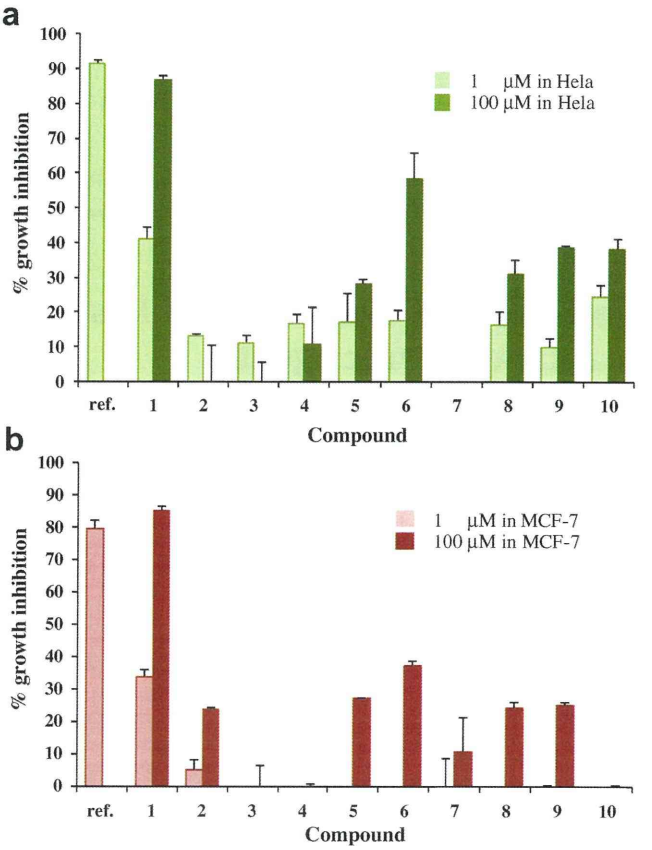

Figure 2. In vitro cytotoxicity effect of 1-(substituted)-3-prop-2-ynylureas at 1 μM and 100 μM against HELA (a) and MCF-7 (b). Doxorubicin at 1 μM was used as reference compound, $n = 3$.

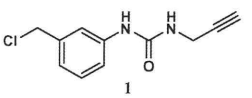

A family of 26 of 1-(substituted)-3-prop-2-ynylureas were next designed by molecular modeling to increase the potency. Flexible ligands were docked to a grid representation of VEGFR2 model derived from crystal structure of the VEGFR2 tyrosine kinase domain in complex with a pyridyl-pyrimidine benzimidazole inhibitor (PDB: 3EWH)[12] using AutoDock4.2[13] (docking experiment and data of all 26 compounds are shown in Supplementary data). Ten compounds were selected based on free energy of binding, hydrogen bond interaction and visual inspection and synthesized and preliminary screened for their cytotoxic effects toward two types of human cancer cell lines, HELA and MCF-7.

Compounds **1–5** were prepared by the reaction between various phenyl isocyanates and propargylamine. The synthetic route is illustrated in Scheme 1.[14,15] Various phenyl isocyanates were prepared in situ via Curtius rearrangement of corresponding acyl azides before reacting with propargylamine to give 1-(substituted)-3-prop-2-ynylureas **1–5**. Briefly, acyl azides were prepared from the corresponding benzoic acids with diphenylphosphoryl azide (DPPA) in the presence of triethylamine in an appropriate solvent. Then, acyl azides were heated at 100 °C to achieve the corresponding isocyanates that were subsequently reacted with propargylamine yielding the desired compounds **1–5**, unoptimized yield: 10–72% (Supplementary data). Compounds **6–10** were synthesized by displacement of chloride of compound **1** with phenols or benzylamines in the presence of K_2CO_3 in one step fashion[16] as illustrated in Scheme 2 (unoptimized yield: 17–80%, synthesis

Table 2
IC_{50} values of the cytotoxicity against HELA, MCF-7

Compound	IC_{50}[a] (μM)	
	HELA	MCF-7
1	1.55	1.48
6	12.26	74.87
7	NA[b]	343.48
8	329.10	49.89
9	339.00	282.90
10	391.50	194.90
Doxorubicin	0.19	0.06

[a] Mean values of three independent experiments are reported.
[b] No activity.

Table 3
IC_{50} against the HUVEC

Compound	IC_{50}[a] (μM)	
	Primary	EA.hy926
1	20	10.54
6	100	78.23
7	50	191.72

[a] Mean values of three independent experiments are reported.

details are shown in Supplementary data). All synthesized compounds were displayed in Table 1.

The synthesized 1-(substituted)-3-prop-2-ynylureas **1–10** were then tested for their cytotoxic effects at 1 and 100 μM against HELA and MCF-7 using MTT assay[17] (Supplementary data). Doxorubicin was used as reference. The compounds that showed growth inhibition over 30% at 100 μM against either cancer cell line were selected for IC_{50} determination.

The initial screening results at two-point concentration of compounds **1–10** were shown in Figure 2. Concentration dependent cytotoxic effects of the compounds in this series against HELA and MCF-7 were observed. Although all compounds demonstrated poor cytotoxic activities comparing to doxorubicin, compound **1** exhibited substantial cytotoxic effect at 100 μM against both HELA and MCF-7 (growth inhibitions of 86.86% and 85.16% for HELA and MCF-7, respectively). Data from cytotoxicity assay of compounds **1–5** suggested that both size and position of substituents on 1-(substituted)-3-prop-2-ynylurea greatly affected on cytotoxic properties of the compounds in this series. Substituents on *para*-position of 1-(phenyl)-3-prop-2-ynylurea decreased cytotoxic effect regardless of the size of substituents as observed in compounds **2** and **3**. Bulky substituent that is, fused ring at position 1 of urea motif (compound **5**) also suppressed cytotoxic potency. The extended structure of compound **1** by displacement of chloride moiety with various phenyl or benzyl via ether- or amine-linker (compounds **6–10**) did not enhance anticancer activity as anticipated, even deteriorated. These emphasized the influence of size of the substituent on phenyl ring at position 1 of urea motif on the cytotoxicity.

Compounds **1**, **6** and **8–10** showed % growth inhibition over 30% at 100 μM against either or both HELA and MCF-7 were selected for the determination for IC_{50}. Among the compounds in this series, compound **1** is most potent compound showing cytotoxic effect on both HELA and MCF-7 with IC_{50} of 1.55 μM and 1.48 μM, respectively (Table 2).

Compounds **1** and **6** showing the best activity against two cancer cell lines were further evaluated for their antiangiogenic effects by tube formation assay, regardless of the considerably high cytotoxic IC_{50} in μM level. Compound **7** with poor activity was included in the assay for comparison. Tube formation assays were performed at non-cytotoxic doses of each compound against the human vein umbilical cell line (HUVEC) (Supplementary data). To identify non-cytotoxic doses for tube formation assay, the in vitro cytotoxicity of compounds **1**, **6** and **7** against HUVEC were performed by MTT assay in the similar fashion as of HELA and MCF-7. IC_{50} values of selected compounds against HUVEC were listed in Table 3.

Tube formation assays of compounds **1**, **6** and **7** were performed. Comparing with control, both compounds **1** and **6**

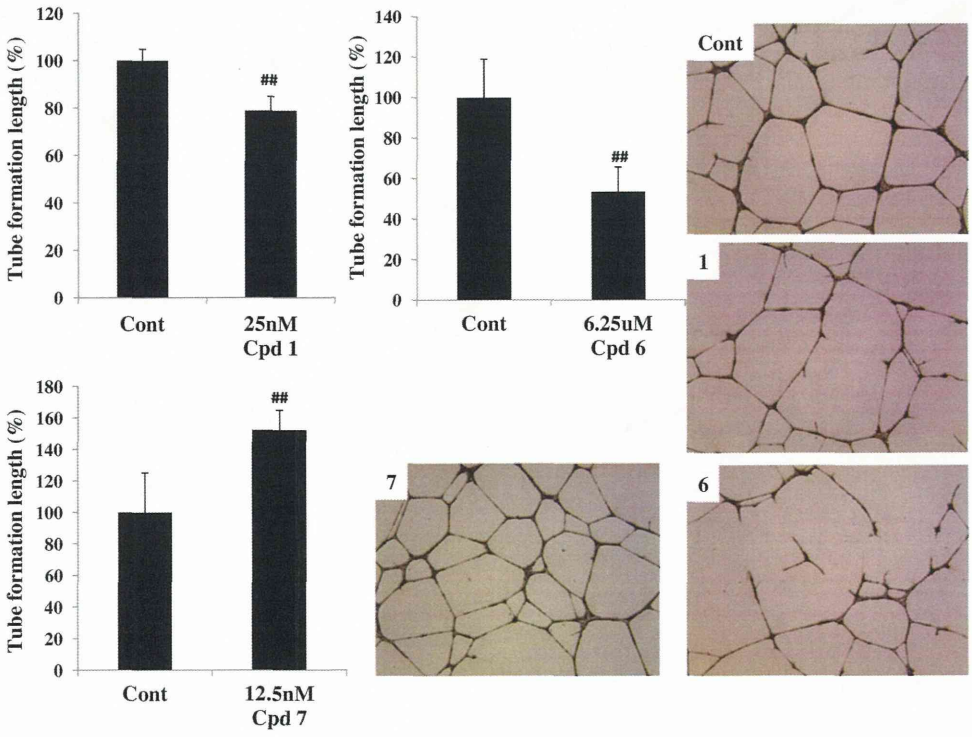

Figure 3. Effect of compounds **1**, **6** and **7** on tube formation comparing with control, $n = 3$, $^{**}p < 0.01$.

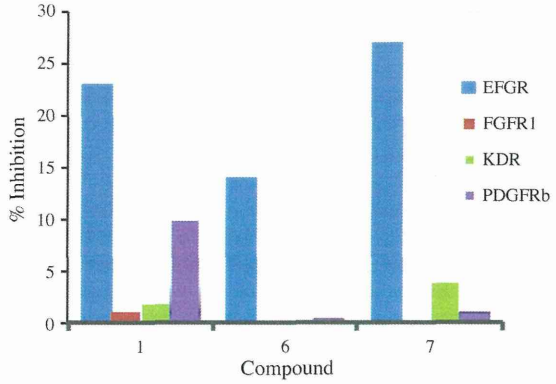

Figure 4. Kinase inhibitory profile at 1 μM against EGFR, FGFR1, VEGFR2 and PDGFRβ tyrosine kinases, % inhibition of erlotinip at 1 μM against EGFR was 98%.

significantly suppressed tube formation of HUVEC. The half maximal effective concentration (EC_{50}) of compounds **1** and **6** against tube formation were found to be 0.26 μM and 17.52 μM, respectively. The observed results from tube formation assay indicated that compounds **1** and **6** possessed antiangiogenic properties against HUVEC. The IC_{50}:ED_{50} ratios for HUVEC of compounds **1** and **6** were 77 and 6, respectively. The antiangiogenic ED_{50} dose of compound **1** was 77 times lower than its cytotoxic IC_{50} dose while that of compound **6** was only 6 times. Apparently, compound **1** did not only possess more potent antiangiogenic activity but also showed safer profile than compound **6**. The minimum effective doses were also determined at the non-cytotoxic dose, compounds **1** and **6** significantly suppressed tube formation of HUVEC at 25 nM and 6.25 μM with 21.18% and 46.47% inhibition, respectively (Fig. 3). Interestingly, compound **7** at non-cytotoxic dose (12.5 nM) showed the increase in tube formation, this compound is currently under investigation for its molecular mechanism.

Compounds **1** and **6** exhibiting significant antiangiogenic activity were evaluated for their effects on tyrosine kinases involving in angiogenesis. In vitro kinase assay of compounds **1** and **6** at 1 μM against VEGFR2, FGFR1, EGFR and PDGFRβ were performed. The levels of phosphorylation of the tyrosine kinase-specific ligand peptides[18–21] at 1 μM of test compounds were measured (Supplementary data). The kinase inhibition profile was displayed in Figure 4.

The tested compounds predominantly inhibited EGFR tyrosine kinase more than other kinases. At 1 μM, compound **1** exhibited significant activity against EGFR and PDGFRβ while compounds **6** and **7** inhibited EGFR tyrosine kinase only. The better cytotoxicity of compound **1** may be due to its ability to inhibit two kinases, EGFR and PDGFRβ.

Since compounds **1** and **6** inhibited EGFR more than the intended VEGFR2, docking of these compounds into ATP binding site of EGFR was performed using AutoDock4.2 to simulate a binding model. The EGFR model was derived from crystal structure of erlotinib bound EGFR obtained from RCSB (PDB: 1M17).[22] Dock poses

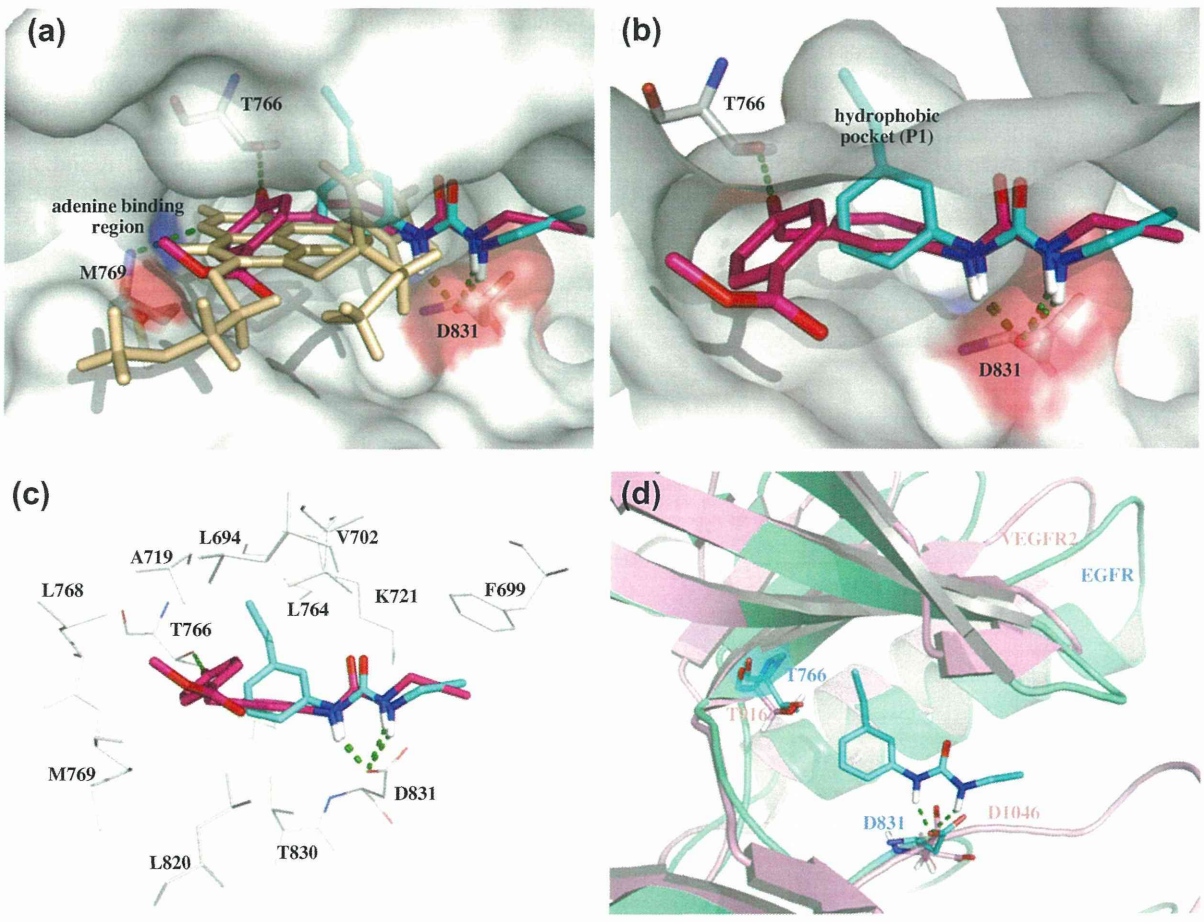

Figure 5. (a) Overlay of binding models of 1-(substituted)-3-prop-2-ylnylurea **1** (cyan), **6** (magenta) and erlotinib (wheat) in kinase domain of EGFR, (b) Overlay of **1** and **6** and their H-bond interactions in the EGFR active site (green dot line), **1** occupied back cavity of ATP binding site of EGFR (P1), (c) binding modes of **1** and **6** displaying interacted amino acid residues, (d) overlay binding model of compound **1** in kinase domain of EGFR (blue) and VEGFR2 (pink), key amino acid residues for H-bond interactions (observed in compounds **1** and **6**) in EGFR (T766 and D831) and in VEGFR2 (T916 and D1046) were illustrated.

Table 4
IC_{50} against A431 cell lines

Compound	IC_{50} (nM)
1	36.00
6	215.50
7	318.00
Erlotinib	55.50

of these compounds were compared with crystal pose of erlotinib as shown in Figure 5a.

EGFR docking results showed that 1-(substituted)-3-prop-2-ynylureas **1** and **6** partially occupied the ATP binding pocket of EGFR whereas erlotinib extensively occupied EGFR kinase domain (Fig. 5a). The partial occupancy may explain the observed low potency in kinase inhibition of these compounds. The 3-chloromethylphenyl substituent of **1** penetrated deeply in the back cavity of the ATP which was a poorly conserved hydrophobic area of the ATP binding site of EGFR.[23] This part of structure was surrounded by the hydrophobic side chains of Phe699, Val702, Ala719, Leu764, Leu820 and the hydrophobic parts of Lys721, Thr766 and Thr830. The urea motif established two hydrogen bonds with the carboxylate of conserved Asp831, a component of DFG motif in the beginning of the activation loop of EGFR which involved in Mg-ATP binding[24] (Fig. 5b). The occupied location of compound **6** was similar to those of **1**, two hydrogen bonds between both *H*N of urea and COOH of Asp831, and an extra hydrogen bond between oxygen atom of ether and O*H* of Thr766, gatekeeper residue of EGFR (Fig. 5b). In addition to Thr766 and Asp831, amino acid residues in hydrophobic pocket that involved hydrophobic interaction included Leu694, Phe699, Val702, Ala719, Lys721, Leu764, Leu768, Met769, Leu820 and Thr830 (Fig. 5c). The binding mode cannot explain the higher potency of **1** over **6** since **6** showed more interacted hydrogen bonds over **1**. The overlay binding mode of **1** in kinase domain of EGFR and VEGFR2 was displayed in Figure 5d. Compound **1** also occupied back cavity of VEGFR2 and was surrounded by the hydrophobic side chains of Val848, Phe1047, Leu1049 and the hydrophobic part of Arg842, Lys868, Asp1046 and Asp1052 (data not shown). The observed hydrogen bond interactions cannot explain the selectivity of **1** against EGFR over VEGFR2 since **1** located in the similar region and bound to DFG motif of both kinases (Asp831 of EGFR and Asp1046 of VEGFR2). However, sequence alignment between EGFR (PDB: 1M17) and VEGFR2 (PDB: 3EWH) by Needle (EMBOSS)[25] showed 28.6% identity and 44.4% similarity suggested that the difference in the hydrophobic component of back cavity observed between EGFR and VEGFR2 might be the key factor controlling the selectivity of **1** and **6** against EGFR over VEGFR2; which appeared to be consistent with the reported notion.[23]

As compounds **1** and **6** were found to inhibit different kinases, especially EGFR, the effect on human epidermoid carcinoma cells A431, EGFR overexpressing cell lines[26–29] was performed (Supplementary data) and the IC_{50} values were reported in Table 4. The IC_{50} values in nM level for EGFR overexpressing A431 cells demonstrated the significance of EGFR kinase inhibition as those for HUVEC were in μM level. The cellular cytotoxicity of **1** was comparable to erlotinip despite of moderate EGFR kinase inhibition, it was possibly due to its ability to inhibit two kinases, EGFR and PDGFRβ.

In summary, a series of novel 1-(substituted)-3-prop-2-ynylureas based on structural modification of compound **1** were prepared to increase the binding capability. The structural modifications of **1** with extended aromatic side chains to increase the binding capability did not enhance tyrosine kinase inhibition nor antiproliferative as expected. Compounds **1** and **6** were cytotoxic against human cancer cells and demonstrated antiangiogenic effect in vitro. In EGFR overexpressing cell line (A431), the cytotoxicity of compound **1** was in nM level comparable to that of erlotinip. The binding mode of **1** from EGFR docking simulation demonstrated that the smaller in size of **1** facilitates and accommodates the hydrogen bond formation in the active sites of the receptors as evidenced by the inhibition of two types of tyrosine kinases (EGFR and PDGFRβ). The urea motif in the compound plays an important role in hydrogen bond interaction with amino acid residues in the active binding site. Terminal alkyne containing urea motif can be considered as new scaffold for further optimization of a potential cancer therapeutic lead.

Acknowledgments

This work was supported by the Royal Golden Jubilee Ph.D. Program (RGJ Grant No. PHD/0229/2547) funded by Thailand Research Fund (TRF) and the commission of Higher Education Thailand (CHE-RG 2551). The authors thank Dr. Benjamin Fraser and Dr. Neil P. Grimster for their valuable advice in some synthesis reactions.

Supplementary data

Supplementary data associated with this article can be found, in the online version, at doi:10.1016/j.bmcl.2012.02.029.

References and notes

1. Zwick, E.; Bange, J.; Ullrich, A. *Trends Mol. Med.* **2002**, *8*, 17.
2. Culhane, J.; Li, E. *US Pharm.* **2008**, *33*, 3.
3. Zwick, E.; Bange, J.; Ullrich, A. *Endocr. Relat. Cancer* **2001**, *8*, 161.
4. Li, H.-Q.; Lv, P.-C.; Yan, T.; Zhu, H.-L. *Anticancer Agents Med. Chem.* **2009**, *9*, 471.
5. Tale, R. H.; Rodge, A. H.; Hatnapure, G. D.; Keche, A. P. *Bioorg. Med. Chem. Lett.* **2011**, *21*, 4648.
6. Zheng, Q.-Z.; Cheng, K.; Zhang, X.-M.; Liu, K.; Jiao, Q.-C.; Zhu, H.-L. *Eur. J. Med. Chem.* **2010**, *45*, 3207.
7. Yao, P.; Zhai, X.; Liu, D.; Qi, B. H.; Tan, H. L.; Jin, Y. C.; Gong, P. *Arch. Pharm. Chem. Life Sci.* **2010**, *343*, 17.
8. Li, H. Q.; Zhu, T. T.; Yan, T.; Luo, Y.; Zhu, H. L. *Eur. J. Med. Chem.* **2009**, *44*, 453.
9. Ahirwar, K. *IJPRD* **2011**, *2*, 209.
10. Drugs@FDA.
11. Rostovtsev, V. V.; Green, L. G.; Fokin, V. V.; Sharpless, K. B. *Angew. Chem., Int. Ed.* **2002**, *41*, 2596.
12. Cee, V. J.; Cheng, A. C.; Romero, K.; Bellon, S.; Mohr, C.; Whittington, D. A.; Bak, A.; Bready, J.; Caenepeel, S.; Coxon, A.; Deak, H. L.; Fretland, J.; Gu, Y.; Hodous, B. L.; Huang, X.; Kim, J. L.; Lin, J.; Long, A. M.; Nguyen, H.; Olivieri, P. R.; Patel, V. F.; Wang, L.; Zhou, Y.; Hughes, P.; Geuns-Meyer, S. *Bioorg. Med. Chem. Lett.* **2009**, *19*, 424.
13. http://autodock.scripps.edu/.
14. Flynn, D. L.; Kaufman, M. D.; Patt, W. C.; Petillo, P. A. USA Patent WO/2008/034008A2, 2008.
15. Spraul, B. K.; Suresh, S.; Jin, J.; Smith, D. W. *J. Am. Chem. Soc.* **2006**, *128*, 7055.
16. Clark, P. G.; Day, M. W.; Grubbs, R. H. *J. Am. Chem. Soc.* **2009**, *131*, 13631.
17. IC_{50} value is the concentration required to inhibit 50% of cell viability by the test compound after exposure to cells.
18. Itokawa, T.; Nokihara, H.; Nishioka, Y.; Sone, S.; Iwamoto, Y.; Yamada, Y.; Cherrington, J.; McMahon, G.; Shibuya, M.; Kuwano, M.; Ono, M. *Mol. Cancer Ther.* **2002**, *1*, 295.
19. Mohammadi, M.; McMahon, G.; Sun, L.; Tang, C.; Hirth, P.; Yeh, B. K.; Hubbard, S. R.; Schlessinger, J. *Science* **1997**, *276*, 955.
20. Weber, W.; Bertics, P. J.; Gill, G. N. *J. Biol. Chem.* **1984**, *259*, 14631.
21. Baxter, R. M.; Secrist, J. P.; Vaillancourt, R. R.; Kazlauskas, A. *J. Biol. Chem.* **1998**, *273*, 17050.
22. Stamos, J.; Sliwkowski, M. X.; Eigenbrot, C. *J. Biol. Chem.* **2002**, *277*, 46265.
23. Zuccotto, F.; Ardini, E.; Casale, E.; Angiolini, M. *J. Med. Chem.* **2009**, *53*, 2681.
24. Hubbard, S. R.; Till, J. H. *Annu. Rev. Biochem.* **2000**, *69*, 373.
25. The tool for pairwise sequence alignment from European Bioinformatics Institute (EMBL-EBI) at http://www.ebi.ac.uk/Tools/psa/emboss_needle.html.
26. Gan, H. K.; Walker, F.; Burgess, A. W.; Rigopoulos, A.; Scott, A. M.; Johns, T. G. *J. Biol. Chem.* **2007**, *282*, 2840.
27. Kwok, T. T.; Sutherland, R. M. *Br. J. Cancer* **1991**, *64*, 251.
28. Rigerike, T.; Blystad, F. D.; Levy, F. O.; Madshus, I. H.; Stang, E. *J. Cell Sci.* **2002**, *115*, 1331.
29. Bravo, R.; Burckhardt, J.; Curran, T.; Müller, R. *EMBO J.* **1985**, *4*, 1193.

A Phagocytotic Inducer from Herbal Constituent, Pentagalloylglucose Enhances Lipoplex-Mediated Gene Transfection in Dendritic Cells

Shinichiro KATO,[a] Keiichi KOIZUMI,*[,a] Miyuki YAMADA,[a] Akiko INUJIMA,[a] Nobuhiro TAKENO,[a] Tsuyoshi NAKANISHI,[b] Hiroaki SAKURAI,[a] Shinsaku NAKAGAWA,[c] and Ikuo SAIKI[a]

[a] *Division of Pathogenic Biochemistry, Institute of Natural Medicine, University of Toyama; 2630 Sugitani, Toyama 930–0194, Japan:* [b] *Laboratory of Hygienics, Gifu Pharmaceutical University; 5–6–1 Mitahora-higashi, Gifu 502–8585, Japan: and* [c] *Department of Biotechnology and Therapeutics, Graduate School of Pharmaceutical Sciences, Osaka University; Suita, Osaka 565–0871, Japan.* Received May 6, 2010; accepted August 19, 2010

Antigen-presenting cells are key vehicles for delivering antigens in tumor immunotherapy, and the most potent of them are dendritic cells (DCs). Recent studies have demonstrated the usefulness of DCs genetically modified by lipofection in tumor immune therapy, although sufficient gene transduction into DCs is quite difficult. Here, we show that *Paeoniae radix*, herbal medicine, and the constituent, 1,2,3,4,6-penta-*O*-galloyl-β-D-glucose (PGG), have an attractive function to enhance phagocytosis in murine dendritic cell lines, DC2.4 cells. In particular, PGG in combination with lipofectin (LPF) enhanced phagocytic activity. Furthermore, PGG enhanced lipofection efficacy in DC2.4 cells, but not in colorectal carcinoma cell lines, Colon26. In other words, PGG synergistically enhanced the effect of lipofectin-dependent phagocytosis on phagocytic cells. Hence, according to our data, PGG could be an effective aid in lipofection using dendritic cells. Furthermore, these findings provide an expectation that constituents from herbal plant enhance lipofection efficacy.

Key words dendritic cell; lipofection; 1,2,3,4,6-penta-*O*-galloyl-β-D-glucose; phagocytosis

Dendritic cells (DCs) play a pivotal role in initiating and controlling the T cell-dependent immune response.[1] Immature DCs, localized in non-lymphoid tissues, have optimal capabilities for antigen uptake, processing and the formation of peptide-major histocompatibility (MHC) complexes. Antigen uptake and some cytokines, for example, in the inflammatory environment, promote their maturation and migration to T cell areas of regional lymphoid tissues, where matured DCs strongly present MHC class I and II restricted peptides to naïve T cells, inducing an immune response and differentiation.[2,3] Because of these properties, DCs have been considered quite attractive immune cells to achieve gene transduction for DNA-based immunization in tumor immunotherapy[4—7] and many gene delivery methods have attempted to optimize transduction and transfection to human and murine dendritic cells.[8—10]

However, despite advances in the understanding of DC biology, the development of genetic immunization strategies using DC-transfected plasmid DNA has been limited by their low transfection efficiencies.[11] Currently, the most efficient method for DC transduction is infection using a viral vector based on poxvirus, lentivirus, and adenovirus,[8,12,13] but viral vectors may be associated with safety concerns and generally require DNA codon optimization to overcome poor gene expression.[14,15] An attractive alternative to vector-mediated delivery into DCs is lipofection, non-viral gene transduction. The main advantages of lipofection are its ability to transfect all types of nucleic acids in a wide range of cell types, its ease of use, reproducibility and low toxicity.[16] Furthermore, recent studies have demonstrated the usefulness of DCs genetically modified by lipofection in tumor immunotherapy,[17] while sufficient gene transduction to DCs is quite difficult.[18] Therefore, it is easily thought that more efficient (DNA-based) DC vaccine therapy could be developed by not only understanding DC immune biology but also finding methods or substances which enhance lipofection efficiency in DCs.

We have sought out immunomodulating compounds derived from herbal medicine or Kampo preparations (formulation) for cancer therapy, especially metastasis.[19,20] In this study, we found that 1,2,3,4,6-penta-*O*-galloyl-β-D-glucose (PGG), which is contained in *Paeoniae radix* (roots of Paeonie lactiflora),[21] enhanced phagocytosis in murine a denndritic cell line, DC2.4, especially in combination with lipofectin (LPF). Lipofectin reagent (LPF; Invitrogen, CA, U.S.A.) is a cationic liposome, mixture of *N*-[1-(2,3-dioleyloxy)propyl]-*n*,*n*,*n*-trimethylammonium chloride (DOTMA) and dioleoyl phosphotidylethanol amine (DOPE) at 1 : 1 (w/w), and is widely used as a device for transfection of RNA, DNA, oligonucleotide and protein.[22—26]

These results motivated us to explore the effect of PGG on DC2.4 cells. PGG is a naturally occurring polyphenolic compound contained in many medical plants[27,28] and a number of studies have reported that PGG exhibits diverse bioactivity, for example, anti-tumor, anti-oxidant, and anti-inflammatory effects.[29] However, the effect of PGG on the phagocytosis of dendritic cells (DCs) has not been investigated, while th effect of polyphenol and tannins (a polyphenol) on phagocytosis and dendritic cells have been investigated well.[30—32] Phagocytosed exogenous antigens complexed with LPF induce high-antigen presentation *via* MHC class I and II and cytotoxic T lymphocytes (CTLs).[33,34] Hence, PGG may be a powerful candidate for tumor immunetherapy because it enhances the phagocytic effect of DC2.4 cells.

On the other hand, we hypothesized that PGG could enhance lipofection efficacy and have a new application for lipofection on DCs because lipofection largely depends on the phagocytic effect,[35] therefore, the present study investigated the effect of PGG on lipofection efficacy in DC2.4 and bone marrow-derived dendritic cells (BMDCs). Moreover, to demonstrate whether the effect of PGG depends on phagocytosis, we also tested the effect on Colon 26, murine colorectal carcinoma cell line. According to our data, the enhancement of lipofection efficacy by PGG was specific for dendritic cells and PGG could be a seed compound of an effective aid

* To whom correspondence should be addressed. e-mail: kkoizumi@inm.u-toyama.ac.jp

for lipofection.

MATERIALS AND METHODS

Reagents AIM-V and Opti-MEM were purchased from Invitrogen (Carlsbad, CA, U.S.A.)/ GIBCO BRL (Grand Island, New York, U.S.A.). The aqueous extraction from *Paeoniae radix* was performed, as previously mentioned.[36] Briefly, about 45 g dried and cut roots were brewed with 900 ml water. Then the filtrate was collected after filtration. The residue was boiled with 800 ml water again and added in the filtrate after filtration. The filtrate was lysophilized. The powder was stored at 4 °C. The concentration used in the experiment was based on the dry weight of the extract (mg/ml). 1,2,3,4,6-penta-*O*-galloyl-β-D-glucose (PGG) was purchased from Toronto Research Chemicals Inc. PGG stock solution, originally dissolved to a concentration of 5 mM in 100% dimethyl sulfoxide (DMSO). Paeoniflorin was purchased from Wako Pure Chemical Industries, Ltd. (Osaka, Japan) Paeoniflorin and Gallic acid (GA) stock solution originally dissolved to a concentration of 10 mM in distillated water. 1,3,6-tri-*O*-galloyl-β-D-glucose (TGG) stock solution originally dissolved to a concentration of 10 mM in 100% DMSO. These all chemical compounds were diluted to the desired concentration in AIM-V or Opti-MEM just before using.

Cell Culture DC2.4 cell, derived from a c57BL/6 immature dendritic cell line, was maintained in RPMI1640 supplemented with 50 μM β-melcaptoethanol. Colon26, derived from BALB/c colorectal cancer, was maintained with RPMI1640 supplemented with 2 mM L-glutamine. All media contained 10% fetal calf serum (FCS), 100 U/ml penicillin and 100 mg/ml streptomycin, and cultures were kept at 37 °C in a humidified atmosphere of 5% CO_2/95% air.

Phagocysosis in DC2.4 Fluorescence isothiocianate (FITC) conjugated-dextran (average molecular weight 40 kDa) was purchased from SIGMA-ALDRICH (St. Louis, MO, U.S.A.) and originally dissolved to a concentration of 10 mg/ml in balanced salt solution (BSS). Phagocytosis in DC2.4 was performed by modification of a previously reported method.[37] In this assay, AIM-V media was used instead of growth media. Briefly, 1×10^5 cells/well were seeded in a 24-well plate (Corning corter) and pre-incubated with PGG for 1.5 h at 37 °C. Pre-treated DC2.4 was phagocytosed in the presence of 10—500 μg/ml FITC-dextran or lipoplex for 1 h at 37 °C, which was made of FITC-dextran and 20 μl Lipofectin (Invitrogen) by co-incubation for 35 min. To inhibit phagocytosis of DC2.4 cells, DC2.4 cells were pre-incubated with wortmannin (final concentration; 5 μM) for 20 min before addition of FITC-dextran. FITC-positive cells were detected by fluorescence microscopy using a Keyence fluorescence microscope. For quantitative determinations of transfection efficiency, fluorescent cells were assessed by fluorescence-activated cell sorting (FACS) using a FACSCalibur flow cytometer (Becton-Dickinson, Mountain View, CA, U.S.A.) and CellQuest software.

Differentiation of Bone Marrow-Derived Dendritic Cells Bone marrow-derived dendritic cells (BMDCs) were differentiated from c57BL/6NCrSlc (9—10-weeks-old specific pathogen free female, Japan SLC (Hamamatsu, Japan)) as reported previously.[38] Differentiated BMDCs were qualified by immunophenotypes and phagocytic activity using FITC-dextran and we used defined BMDCs which express both CD11c and MHC class II more than 70% of total population.

Plasmids The vectors encoding green fluorescent protein (GFP) mutant, pEGFP-N1 and pEGFP-C1, were purchased from Clontech (Palo Alto, CA, U.S.A.). These vectors encode a mutant GFP that contains more than 190 silent nucleotide changes to optimize the coding sequence based on human codon-usage preferences,[39] and mutations at residue 64 (Phe→Leu) and 65 (Ser→Thr), which results in enhanced fluorescence and a single excitation peak at 488 nm.

Lipofection and Transgenes Expression Lipofection using a lipofectin reagent was performed by following the modified instructions of the manufacture. One day before transfection, 2×10^5 cells were seeded in growth media, and nearly 60% confluent cells were used for lipofection. Four microliters of lipofectin reagent was diluted in 100 μl Opti-MEM in one tube and incubated for 30 min at room temperature. Meanwhile, 2—4 μl pEGFP-N1 (1 μg/μl) and pEGFP-C1 (1 μg/μl) (Clontech) were diluted in 100 μl Opti-MEM in another tube separately for 15 min at room temperature. The transfection reagents and plasmid solution were then mixed and incubated at room temperature based on the manufacturer's instructions. Cells were familiarized with Opti-MEM for 30 min before lipofection. Eight-hundred microliters of Opti-MEM were added to the mixed solution (finally 200 μl+800 μl), then after removal of the conditioned Opti-MEM, cells were added to transfection solutions (1 ml) and incubated for 5 h. After lipofection for 5 h, transfection solution was replaced with growth media. In PGG-assisted lipofection, PGG was used for incubation of lipoplex throughout lipofection. Twenty-four hours following lipofection, enhanced green fluorescent protein (EGFP)-positive cells were detected and quantified by the same methods as for the phagocytosis of DC2.4.

Flow Cytometric Analysis and Immunophenotypic Analysis After removal of the supernatant, cells were split off using 0.13% trypsin and ethylenediaminetetraacetic acid (EDTA), pelleted by centrifugation, resuspended in phosphate buffered saline (PBS) containing 2% FCS to a final density of -5×10^6 cells/ml, and filtered through a nylon membrane to remove cell aggregates. Flow cytometry for EGFP and propidium iodide (PI) fluorescence were performed using a FACSCalibur (BD Bioscience). For immunophenotypic analysis of DC2.4 cells, split cells were suspended in FACS buffer ($0.5—1\times10^6$ cells/50 μl), containing PBS in 0.02% NaN_3 (w/v) and 2% FCS (v/v). Cells were first incubated with an antibody against FcRg (clone 2.4G2) for 5 min and then labeled with antibodies against CD80 (clone 16-10A1), CD86 (clone GL1), MHC class I (clone 28-14-8) and MHC class II (clone M5/114.15.2) for 30 min. All polyethylene (PE)-conjugated mAb were acquired from BD Biosciences.

Statistical Analysis Three means (±1 S.D.) were composed using analysis of variance (ANOVA) (Figs. 1, 3). Two means (±1 S.D.) were composed using the unpaired Student's *t*-test (two tailed) (Figs. 2, 4). A p value of less than 0.05 was considered significant.

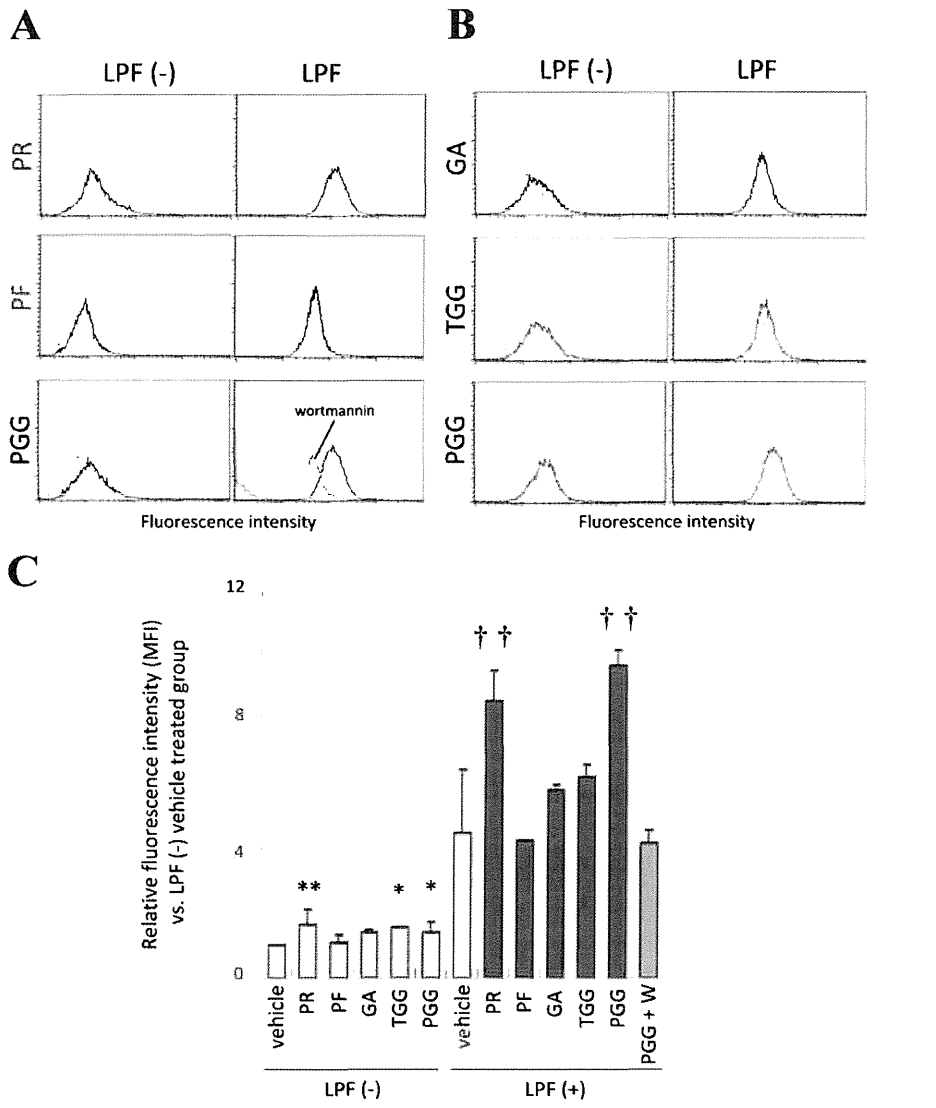

Fig. 1. Ability of 1,2,3,4,6-Penta-*O*-galloyl-*β*-D-glucose (PGG) to Phagocytose into DC2.4

After pre-incubation with (A) 1 mg/ml *Paeoniae radix* (PR), 10 mM Paeoniflorin (PF) or 10 mM PGG and (B) 10 mM gallic acid (GA), 10 mM 1,3,6-tri-*O*-galloyl-*β*-D-glucose (TGG) or 10 mM PGG for 1.5 h, DC2.4 phagosytosed for 1 h at 37 °C in the presense of 250 mg/ml FITC-dextran combined without (left) or with (right) Lipofectin (LPF). Phagocytosed DC2.4 were analyzed by flow cytometer. Filled profile, non-treated cells as control; gray dotted line, FITC-dextran without preincubation with indicated compounds; black line, FITC-dextran with preincubation with indicated compounds, FITC-dextran with preincubation with PGG and 5 μM wortmannin (abbreviation; W) to inhibit phagocytosis. Data are representative of at least two independent experiments. (C) Relative mean fluorescence intensity (MFI) as phagocytic activity was assessed by flow cytometry. Data are presented as the means±S.D. of at least two independent experiments. $*p<0.05$, $**p<0.01$, *vs.* LPF (−) vehicle group, $\dagger\dagger p<0.01$, *vs.* LPF (+) vehicle group by analysis of variance (ANOVA) with Bonferroni correction.

RESULTS AND DISCUSSION

Phagocytosis in DC2.4 Cells Was Enhanced by 1,2,3,4,6-Penta-*O*-galloyl-*β*-D-glucose (PGG) Recently, we found that the ability of *Paeonie radix* (aqueous extractions) to engulf FITC-dextran into DC2.4 cells occurred in an FITC-dextran and *Paeonie radix* (PR) (Figs. 1A, C). To identify which chemical compounds enhanced engulfment in DC2.4 cells from *Paeonie radix*, we tested the effect of paeoniflorin (PF) and PGG, contained in PR,[27] on incorporation of FITC-dextran in DC2.4 cells. Of these compounds, PGG enhanced engulfment in DC2.4 cells at the same level as PR, while PF, which is the major compound contained in PR, hardly enhanced engulfment (Fig. 1A). PGG had little effect on engulfment with FITC-dextran alone but engulfment was apparently enhanced with the FITC-dextran/lipofectin (LPF) complex (Fig. 1C). The effect was cancelled by wortmannin, a phagocytosis inhibitor,[40] suggesting that the increase of intracellular FITC-dextran depended on the enhancement of phagocytic activity (Figs. 1A, C). This means that PGG synergistically enhances phagocytosis in combination with LPF in DC2.4 cells. In this property, PGG is utilized for lipofection using LPF. Furthermore, we also found the importance of the chemical structure of PGG in the enhancement of phagocytosis in DC2.4 cells (Figs. 1B, C). PGG has five ester bonds formed between the hydroxyl group of the glucose backbone and the carboxyl group of gallic acid (GA).[29] 1,3,6-Tri-*O*-galloyl-*β*-D-glucose (TGG), which has three ester bonds, enhanced the phagocytosis of DC2.4 in the absence of LPF and had a tendency to enhance